Lithos 272–273 (2017) 69–83

Contents lists available at ScienceDirect

Lithos

journal homepage: www.elsevier.com/locate/lithos

The pre-Atlantic Hf isotope evolution of the east Laurentian continental margin: Insights from zircon in basement rocks and glacial tillites from northern New Jersey and southeastern New York

N. Alex Zirakparvar [a,*], Jacob Setera [b], Edmond Mathez [a], Jill Vantongeren [b], Ryanna Fossum [c]

[a] Dept. Earth & Plan. Sci., American Museum of Natural History, Central Park West at 79th St, New York, NY 10024, United States
[b] Dept. Earth & Plan. Sci., Rutgers, The State University of New Jersey, Wright-Rieman Laboratories, 610 Taylor Road, Piscataway, NJ 08854-8066, United States
[c] Geology Dept., Oberlin College, 2 W. Lorain St., Carnegie Building, Rm. 403, Oberlin, OH 44074, United States

ARTICLE INFO

Article history:
Received 8 June 2016
Accepted 18 November 2016
Available online 28 November 2016

Keywords:
Zircon
U–Pb geochronology
Hf isotopes
Crustal evolution
Laurentian margin

ABSTRACT

This paper presents laser ablation U–Pb age and Hf isotope data for zircons from basement rocks and glacial deposits in northern New Jersey and southeastern New York. The purpose is to understand the eastern Laurentian continental margin's Hf isotope record in relation to its geologic evolution prior to the opening of the Atlantic Ocean. The basement samples encompass a Meso- to Neoproterozoic continental margin arc, an anatectic magmatic suite, as well as a Late Ordovician alkaline igneous suite emplaced during post-orogenic melting of the lithospheric mantle. Additional samples were collected from terminal moraines of two Quaternary continental ice sheets. Across the entire dataset, zircons with ages corresponding to the timing of continental margin arc magmatism (~1.4 Ga to ~1.2 Ga) have positive $\varepsilon_{Hf(initial)}$ values that define the more radiogenic end of a crustal evolution array. This array progresses towards more unradiogenic $\varepsilon_{Hf(initial)}$ values along a series of low $^{176}Lu/^{177}Hf$ (0.022 to 0.005) trajectories during subsequent anatectic magmatism (~1.2 Ga to ~1.0 Ga) and later metamorphic and metasomatic re-working (~1.0 Ga to ~0.8 Ga) of the continental margin arc crust. In contrast, nearly chondritic $\varepsilon_{Hf(initial)}$ values from the Late Ordovician alkaline magmas indicate that the Laurentian margin was underlain by a re-fertilized mantle source. Such a source may have developed by subduction enrichment of the mantle wedge beneath the continental margin during the Mesoproterozoic. Additionally, preliminary data from a metasedimentary unit of unknown provenance hints at the possibility that some of the sediments occupying this portion of the Laurentian margin prior to the Ordovician were sourced from crust older than ~1.9 Ga.

1. Introduction

All of Earth's continents have been affected by numerous episodes of magmatism, metamorphism, and metasomatism (e.g., Hawkesworth et al., 2010), making it difficult to decipher how they were assembled. One problem is to distinguish geochemical characteristics reflecting processes that occurred during the formation of cratons from processes that occurred subsequently. In this regard, the technique of combining zircon U–Pb age and Hf isotope data, both sampled via laser ablation, for single zircon crystals has arguably proven to be one of the more successful means of unraveling complex geologic histories. The widespread application of this technique to a variety of petrologic questions has generated over 40,000 individual initial (at the time of crystallization) zircon epsilon Hf ($\varepsilon_{Hf(initial)}$) values across the literature (Roberts and Spencer, 2015).

When examined on a global-scale, zircon $\varepsilon_{Hf(initial)}$ values have been used to understand the Hf isotope evolution of Earth's continental crust (Condie et al., 2009; Guitreau et al., 2012; Roberts and Spencer, 2015). These data raise two outstanding questions: (1) What are the geologic processes behind the zircon Hf isotope crustal evolution arrays commonly observed in craton-scale datasets? (e.g. Naeraa et al., 2012) and (2) How does continental margin arc magmatism affect the Lu-Hf isotope systematics of the margin's lithospheric mantle? (Laurent and Zeh, 2015; Zirakparvar et al., 2014) The answers to these questions lie partly in our understanding of how subduction-related arc magmatism and subsequent anatectic melting modify the Lu-Hf isotope systematics of the crust and upper-mantle at active continental margins. They also lie in understanding how the process whereby juvenile material is accreted to, and undergoes re-working along, continental margins is recorded in the zircon Hf isotope data.

One way study these questions is to define trends and relationships in age vs ε_{Hf} space as a function of known tectonic histories. This can be done in the case of the New Jersey Highlands (NJH), which exposes the mid- to lower crust of a continental margin magmatic arc system that formed along the eastern edge of Laurentia during the Mesoproterozoic (Volkert and Drake, 1999; Volkert et al., 2010). This continental margin was intruded by magmas derived from the lithospheric mantle ~0.8 Ga following the cessation of subduction-related continental arc magmatism. In this way, the NJH terrane and surrounding region provide a natural

* Corresponding author.
E-mail address: nzirakparvar@amnh.org (N.A. Zirakparvar).

http://dx.doi.org/10.1016/j.lithos.2016.11.023
0024-4937/

laboratory for evaluating how the Hf isotope systematics of a continental-margin magmatic arc, including the lithospheric mantle beneath it, behaved through time.

This study uses laser-ablation-inductively coupled plasma mass spectrometry (LA-ICP-MS) to acquire U–Pb ages and Hf isotope compositions for adjacent analytical volumes within single zircon grains. The zircons were extracted from samples representing the Laurentian margin's Mesoproterozoic arc crust and Late Ordovician lithospheric mantle melts that subsequently intruded it. The dataset is augmented by a similar data from samples recovered from the region's Quaternary glacial deposits. This dataset is used to: 1) Understand the Lu-Hf systematics of juvenile arc magmatic crust from its production during the Mesoproterozoic followed by its anatectic re-working up to ~0.8 Ga, 2) Document the existence of a subduction enriched lithospheric mantle source for alkaline magmas that intruded the former arc crust during Ordovician time, and 3) Address regional geodynamic questions that establish a framework for future investigation of the continental margin's tectonic history.

2. Regional geologic and tectonic history

The plate-boundary scale bedrock geology of eastern North America can be divided into two broad groups on the basis of differing tectonic histories and rock types. One group encompasses the Triassic-Jurassic syn-rift volcanic and sedimentary deposits that occupy the numerous basins formed during the opening of the Atlantic Ocean (Fig. 1a) and also includes the post-rift sedimentary sequences on the North American passive margin. A second group constitutes the older, high-grade metamorphic and magmatic basement rocks that record the region's history of continental arc magmatism, terrane accretion, continent-continent collision, and post-orogenic magmatism (Fig. 1a).

In eastern North America, basement rocks can be further subdivided on the basis of tectonic history into the Grenville Province of eastern Ontario and Quebec, the Adirondack Grenville Inlier of northern New York, and the Appalachian Mesoproterozoic Inliers (Fig. 1a). The latter define a ~2500 km long belt extending from northwestern Georgia to Central Vermont (Fig. 1a). Pre-rift basement in eastern North America also encompasses the remnants of the numerous exotic terranes accreted to the continental margin throughout the Paleozoic, as well as the suture zones between these terranes. The interested reader is referred to reviews of Bartholomew and VanArsdale (2013), McLelland et al. (2010), and Withjack et al. (2013).

Focusing on the regional geology and tectonic history of the study area (Fig. 1b), samples were collected in northern New Jersey and southeastern New York (Fig. 1b). In northern New Jersey, high-grade metamorphic rocks of the New Jersey Highlands (NJH) terrane are separated from a much younger sequence of Triassic-Jurassic aged syn-rift sedimentary and volcanic rocks occupying the Newark Basin by the Ramapo Fault (Figs. 1b and 2). The NJH terrane has most recently been studied by Volkert et al. (2010), who performed a comprehensive SHRIMP U–Pb zircon and monazite dating campaign in order to constrain the timing of major tectonic, magmatic, and metamorphic events preserved in the region.

The New Jersey Highlands constitute one of the more than 13 known Mesoproterozoic Appalachian Inliers (McLelland et al., 2010), but the coverage of high-precision U–Pb ages in the NJH terrane supersedes that of the other terranes. On the basis of SHRIMP U–Pb age dating of monazite and zircon along with geologic and geochemical data, Volkert et al. (2010) defined three main units. One encompasses the Wanaque and Losee suites, which are composed of dacitic, tonalitic, and dioritic gneisses with magmatic ages ranging from 1366 ± 9 Ma to 1248 ± 5 Ma. These rocks are interpreted as the mid- to lower crust of the southern continuation of a Mesoproterozoic magmatic arc system that formed along the eastern margin of Laurentia in response to subduction of oceanic crust from ~1.4 Ga to ~1.2 Ga.

The second unit consists of metamorphosed supracrustal rocks that formed inboard of the Mesoproterozoic arc system, and the third unit consists of anatectic magmas (i.e., not subduction related) that intruded the arc crust in two pulses at ~1188 Ma and ~1027 Ma (Volkert et al., 2010). The rocks in the NJH terrane were also pervasively metamorphosed to the granulite facies between 1045 and 1024 Ma, as revealed by the U–Pb ages of overgrowths on monazite and zircon. Slightly

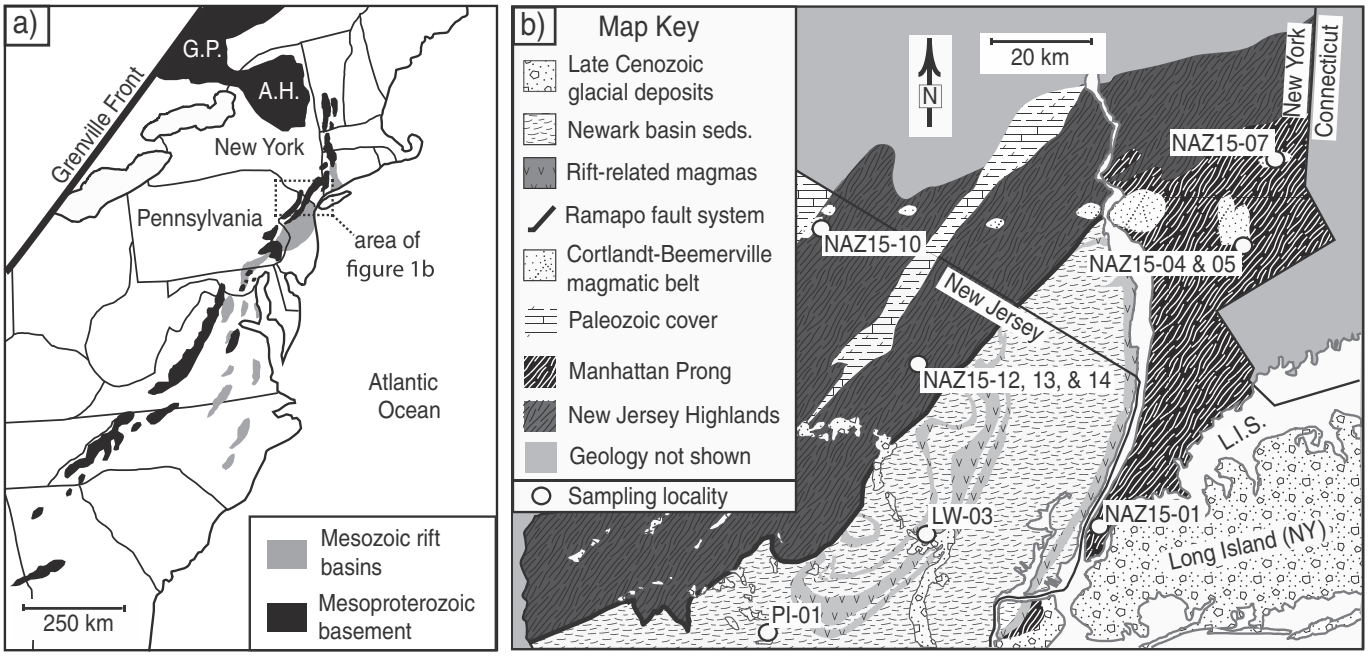

Fig. 1. Schematic maps illustrating: a) The location of Mesoproterozoic inliers situated along the eastern continental margin of the United States (after McLelland et al., 2010). Also shown is the Grenville Province (G.P.), Adirondack Highlands (A.H.) and approximate locations of major Triassic-Jurassic aged rift basins (after Withjack et al., 2013), and b) The regional-scale geology of the study area (modified after Drake et al., 1996) with the locations of analyzed samples.

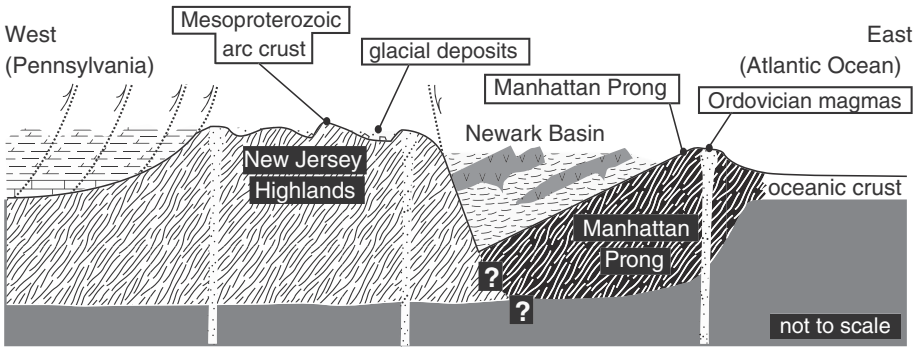

Fig. 2. Schematic cross-section from west to east across the study area showing relations among the Mesoproterozoic arc crust in the New Jersey Highlands, the Late Ordovician alkaline magmas in the Cortlandt-Beemerville magmatic belt, the Manhattan Prong, and the Late Cenozoic glacial deposits overlying all of these lithostratigraphic subdivisions.

younger overgrowths with ages ranging from 996 to 989 Ma have been interpreted to reflect poorly understood thermal disturbances and hydrothermal activity associated with U-Th-REE mineralization.

A prominent regional feature is a tectonic boundary separating allochthonous Mesoproterozoic rocks of the eastern Laurentian continental margin and authochthonous rocks accreted to this margin during the Taconic and Acadian orogenies. In the study area, the younger allochthonous rocks form the Manhattan Prong east of the Hudson River. The Manhattan Prong consists of schist, marble, and quartzite with inferred Cambrian to Ordovician protolith ages (Paige, 1955). The metasedimentary units are of unknown provenance and uncomfortably overly ~600 Ma old gneissic basement of magmatic origin (Mose and Hayes, 1975).

K-Ar mineral and Rb-Sr whole-rock dates for the Manhattan Prong rocks suggest that it experienced complete recrystallization and partial melting between ~360 Ma (Long and Kulp, 1962) and ~380 Ma (Mose et al., 1975). The Manhattan Prong has long been inferred to possess a different, but poorly understood, tectonic history compared to the NJH (Hall, 1975; Long and Kulp, 1958; Merguerian, 1983; Paige, 1955; Prucha, 1956). It may represent sediments shed off the continental margin prior to metamorphism during the Taconic or Acadian orogenies, or it may have been an exotic terrane.

Another important regional geologic feature is the Late Ordovician Cortlandt–Beemerville belt, a series of mafic to intermediate bodies that extend westward from the New York–Connecticut border into New Jersey (Fig. 1b). Ratcliffe (1981) suggested that this belt intruded during the Late Ordovician immediately following collision-related compression associated with the Taconic orogeny, a hypothesis supported by recent SHRIMP zircon and TIMS titanite U–Pb dates indicating ages from 446 ± 2 Ma to 452.3 ± 4.5 Ma (Ratcliffe et al., 2012). The Beemerville magmatic complex, at the western end of the belt, consists of several large bodies of nepheline syenite diatreme pipes and dikes of lamprophyre, tiguanite, and phonolite (Eby, 2004). Other intrusions in the belt also display alkaline bulk compositions, suggesting that they were generated by melting of the lithospheric mantle (Ratcliffe, 1981).

Following the intrusion of the Late Ordovician magmatic belt, the next major geologic event recorded in the region is basaltic magmatism and rift basin development associated with the opening of the Atlantic Ocean. In the study area, this phase of activity is highlighted by ~201 Ma U–Pb zircon and baddeleyite ages from the Palisades and Gettysburg basaltic sills (Blackburn et al., 2013; Dunning and Hodych, 1990), which are intercalated with rift-basin sediments in the Newark basin (Fig. 1a). In northern New Jersey, much of the bedrock cover is composed of Late Cenozoic glacial deposits that were transported into the area from the north during three distinct glaciations. The most widespread and best-preserved deposits are those of the late Wisconsinan glaciation. In northern New Jersey ^{14}C ages for materials within and on-top of the late Wisconsinan deposits range from 29.6 to 20 Ka (calendar years) (table 1 in Stone et al. (2002)).

The underlying deposits associated with the other two glaciations are only preserved to the south of the terminal moraine associated with the late Wisconsinan glaciation. Deposits associated with the next youngest glaciation (estimated to be between 160 to 180 ka; Stone et al. (2002)) are restricted to a narrow band, whereas the deposits associated with the oldest glaciation are somewhat more widespread in the study area. While the latter are not exceptionally well preserved or exposed, they do occur over a wide area and have been correlated with pre-Illinoian deposits in Pennsylvania. These pre-Illinoian deposits have been tentatively assigned an age of ~850 ky (Stone et al., 2002).

3. Samples

Samples were collected of NJH Mesoproterozoic arc-related rocks to document the Hf isotope record of long-lived continental arc magmatism, and of the younger igneous bodies to establish the composition of their lithospheric source beneath the arc crust. Samples were also collected of the Manhattan Prong to provide additional constraints on the Hf isotope composition of the regional basement, of which little is known. Finally, samples from glacial deposits were collected to augment the data from the rock samples in relation to the Hf isotope systematics of the broader continental margin.

3.1. Samples from the Mesoproterozoic arc crust

The three NJH samples are strongly foliated quartz-oligoclase gneisses belonging to the Losee Suite (Volkert et al., 2010) collected in a 5-m^2 area of fresh bedrock exposed at the southern end of Split Rock Reservoir in Boonton Township (Electronic Appendix A). The rocks are composed of oligoclase–andesine, quartz, hornblende, hypersthene, biotite, and magnetite but display considerable heterogeneity on outcrop scale and grade locally into meter-scale zones of hypersthene dominated quartz-plagioclase gneiss. These characteristics are consistent with the description of the Losee Suite in Volkert (2012) and Volkert et al. (2010). Sample NAZ15-12 is the magnetite-rich variant, sample NAZ15-13 the hypersthene-dominated gneiss, and sample NAZ15-14 the oligoclase-quartz-dominated gneiss.

3.2. Samples from the Late Ordovician magmatic belt

Three of the intrusions in the Late Ordovician aged Cortlandt-Beemerville magmatic belt were sampled. Sample NAZ15-10 is a nepheline syenite collected in the Beemerville Complex from the western end of the belt. It was collected from sub-outcrop at the southern flank of the Rutan Hill diatreme (Eby, 2004). Ratcliffe et al. (2012)

reported a TIMS U–Pb titanite age from nepheline syenite elsewhere in the Beemerville Complex of 447 ± 2 Ma.

Samples NAZ15-04 (augen gneiss) and NAZ15-05 (monzonite) were collected <5 m apart from an exposure of the Bedford Complex, in the eastern part of the belt (Alavi, 1975). Elsewhere in the Bedford Complex, Ratcliffe et al. (2012) reported a monzonite SHRIMP U–Pb zircon age of 452.3 ± 4.5 Ma, with inherited cores ranging in age from 1.3 to 1.1 Ga. In addition, a monzodiorite (NAZ15-07) was collected from the Peach Lake Complex (Henry, 1997). Ratcliffe et al. (2012) reported a SHRIMP U–Pb age of 449.7 ± 4.3 Ma for monzodiorite elsewhere in the Peach Lake Complex.

3.3. Sample from the Manhattan Prong

A sample of schist (NAZ15-01) was collected from the tailings pile of an excavation on West 76th St in Manhattan, New York City. It is a coarse grained muscovite-quartz-garnet schist that is similar in texture, mineralogy, and appearance to the large outcroppings of schist that occur in nearby Central Park.

3.4. Glacial tillite samples

Sample LW-03 was collected from an exposure of the late-Wisconsinan Rahway Till (Stanford, 2005) that crops out in a steep embankment above the Rahway River in Essex County, NJ. The sample is a reddish-brown, sandy silt containing ~10% subrounded and sub-angular pebbles and cobbles as well as ~1% subrounded boulders. The bulk of clasts consisted of (in order of decreasing proportions) granitoid and gneiss, basalt, purple sandstone and conglomerate. None of the clasts have thick weathering rinds.

Sample (PI-01) was collected from an exposure in an area mapped as pre-Illinoian Port Murray Formation tillite (Stone et al., 2002). The locality is the steep wall of a stream valley on the southern flank of a broad hilltop ~5 km north of Lebanon, NJ. The sample consists of yellowish-brown, sandy clayey silt with many (~15%) subrounded to subangular pebbles and cobbles. Clasts (in order of decreasing abundance) were predominantly gray and white gneiss, red and purple sandstone, and basalt. All of the clasts have thick (>0.5 in. thick) weathering rinds.

4. Methods

4.1. Zircon separation and preparation

In order to obtain zircon separates, rock samples were crushed and washed prior to sieving. The un-lithified nature of the tillite samples did not warrant crushing, so these samples were instead sieved directly under running water to liberate the heavy mineral fraction from the muddy matrix. Once these initial steps were performed, the size-classified (<250 μm) materials from each sample were panned in clean water to remove the bulk of the material. Fe-rich phases were removed from these pan concentrates by the use of a Nd-hand magnet prior to the use of methylene iodide to obtain a non-magnetic heavy mineral concentrate. The concentrates were washed in warm ~2 M HCL prior to being mounted on double-sided tape. The grains were left unpolished to allow for a depth profiling approach to the U–Pb and Hf analyses (e.g. Zirakparvar, 2015). Prior to the U–Pb and Hf analyses, an EDS detector coupled to a Hitachi S-4700 Field Emission SEM at the American Museum of Natural History was used to confirm the presence of zircon.

4.2. U–Pb analyses

The U–Pb analyses were performed at Rutgers University using a Photon Machines 193 nm laser ablation system coupled to a Thermo iCapQc™ mass spectrometer. The laser was run at 50% power and 10 Hz resulting in a fluence of 4.25 J/cm^2 at the zircon surface. The laser spot size was 35 μm in diameter with ablated material carried to the plasma via Helium gas. For each analysis, the iCapQc™ was set-up to acquire data for 220 sweeps with a 10 millisecond per isotope dwell time while the laser was fired for 30 s. Background data were collected immediately prior to each zircon analysis using the same instrumental conditions but without firing the laser. Washout time between the end of an analysis and the start of the next background was approx. 1 min. Data processing was performed using the Iolite software package.

The zircon standard 91500 (Wiedenbeck et al., 1995) was the primary one used during the session and was run after every 5 to 7 unknowns. It was analyzed a total of 52 times, yielding a weighted mean $^{206}Pb/^{238}U$ age of 1062.2 ± 2.5 Ma (2σ; MSWD = 2.2) and weighted mean $^{207}Pb/^{206}Pb$ age of 1057 ± 23 Ma (2σ; MSWD = 5.3). The results from the 91500 standard were used to apply a final fractionation correction to the unknowns via a bracketing approach. The zircon standards Plešovice, Mud Tank, and R33 (Fisher et al., 2014a) were also run during the session and were processed in the same manner as the unknowns. The Plešovice (Slama et al., 2008) standard was run a total of 73 times, yielding a weighted mean $^{206}Pb/^{238}U$ age of 343.4 ± 2.5 Ma (2σ; MSWD = 15) and a weighted mean $^{207}Pb/^{206}Pb$ age of 328 ± 20 Ma (2σ; MSWD = 3.8). The Mud Tank standard was run 8 times, yielding a weighted mean $^{206}Pb/^{238}U$ age of 748 ± 13 Ma (2σ; MSWD = 8.9) and a weighted mean $^{207}Pb/^{206}Pb$ age of 577 ± 40 Ma (2σ; MSWD = 1.3). The R33 standard was run 4 times, yielding a weighted mean $^{206}Pb/^{238}U$ age of 411 ± 19 Ma (2σ; MSWD = 30) and a weighted mean $^{207}Pb/^{206}Pb$ age of 422 ± 43 Ma (2σ; MSWD = 1.4).

4.3. Hf isotope analyses

The Lu-Hf isotope compositions were measured using a New Wave® UP 193 FX excimer laser ablation (LA-) system coupled to a Thermo-Finnigan NeptunePlus® multi collector-inductively coupled plasma-mass spectrometer (MC-ICP-MS) in the Lamont Doherty Earth Observatory of Columbia University—AMNH ICP-MS laboratory. The laser was operated at 10 Hz and 70% power with a 50 μm spot size, resulting in a ~11.5 J/cm^2 fluence and a 2.3 GW/cm^2 irradiance at the zircon surface. The zircon surface was ridded of any contaminants using a 3 s pre-ablation prior to data collection. This was followed by the acquisition of 60 cycles (each with 1.049 s integration time) of data. The NeptunePlus® cup configuration was ^{171}Yb on L4, ^{172}Yb on L3, ^{173}Yb on L2, ^{175}Lu on L1, $^{176}Hf + Lu + Yb$ on the center cup, ^{177}Hf on H1, ^{178}Hf on H2, and ^{179}Hf on H3. Blank corrections were determined by collection of a background using these parameters every four to five zircon analyses.

Hf isotope instrumental mass bias was determined using the measured $^{179}Hf/^{177}Hf$ ratio and a true $^{179}Hf/^{177}Hf$ of 0.7325 (Patchett and Tatsumoto, 1980; Patchett et al., 1981), with atomic masses of 178.945815 and 176.94322, respectively (Baum et al., 2002). Instrumental mass bias (ß) for the Yb isotopes was initially determined by using the measured $^{173}Yb/^{171}Yb$ ratio and a true $^{173}Yb/^{171}Yb$ of 1.132685 (Chu et al., 2002), with atomic masses of 172.938207 and 170.936322, respectively (Baum et al., 2002). However, at low ^{171}Yb signals (e.g. <0.01 V), Cecil et al. (2011) have shown that it is not possible to accurately constrain ßYb. Further complicating the issue of accurately determining ßYb is the fact that the NeptunePlus® has an interface pressure that is more than an order of magnitude lower than its predecessor instrument (Bouman et al., 2009). The low interface pressure affects the accurate determination of ß factors, with the magnitude of the effect being highly sporadic, element specific, and partly dependent on the selection of the sample and skimmer cones as well as the composition of the carrier gas (Hu et al., 2012).

Therefore, an empirically constrained ßYb (as opposed to one directly determined during the analysis) was used for calculation of isobaric interferences of ^{176}Yb on ^{176}Hf and to determine $^{176}Yb/^{177}Hf$. This empirical ßYb was obtained by examination of the relationship between the

average ^{171}Yb signal and final calculated ^{176}Hf/^{177}Hf ratio for individual analyses of the R33 zircon standard, which has a variable Yb content, as functions of different relationships between ßYb and ßHf. For the relationship ßYb = ßHf and the instrument used in this study, there is typically a large overcorrection of the ^{176}Hf/^{177}Hf ratio at relatively high ^{171}Yb intensities. Zirakparvar et al. (2014) and Zirakparvar (2015) have shown that this overcorrection does not exist when ßYb = 0.945 × ßHf. Therefore, the relationship ßYb = 0.945 × ßHf was applied to the interference corrections for all analyses of the standards and unknowns. This approach was tested by repeated analysis of the R33 standard during this study as well.

The assumption that ßLu = ßHf was used to calculate the isobaric interference of ^{176}Lu on ^{176}Hf and in the calculation of ^{176}Lu/^{177}Hf. Isobaric interferences on the ^{176}Hf signal from ^{176}Lu and ^{176}Yb were determined using the peak stripping approach described by Fisher et al. (2011), using the atomic masses for the relevant isotopes reported by Baum et al. (2002) and true ^{176}Yb/^{171}Yb, ^{176}Lu/^{175}Lu, and ^{176}Yb/^{173}Yb of 0.901821, 0.02655, and 0.79618, respectively (Vervoort et al., 2004). Background corrections, mass bias determinations, and isobaric interference corrections were applied for each cycle in the 60 cycle block, with a pre-screening of the block to remove cycles where the laser had passed through the zircon grain or penetrated an inclusion. Once all of these corrections were performed, isotope ratios from each line were averaged together. The 2σ standard error of this average is taken to be the uncertainty for each individual analysis (the 'within run error').

The zircon standards Plešovice, MudTank, R33, 91500, and Penglai (Li et al., 2010) were measured throughout this study, and the following short-term (e.g. during this study's Hf isotope analytical session) averages were obtained (where n = # of analyses): Plešovice: n = 55, ^{176}Hf/^{177}Hf = 0.282458 ± 17 (2σ population standard deviations), εHf $_{(present)}$ = −11.5 ± 0.6; Mud Tank: n = 9, ^{176}Hf/^{177}Hf = 0.282492 ± 27, εHf $_{(present)}$ = −10.3 ± 0.9; R33: n = 15, ^{176}Hf/^{177}Hf = 0.282721 ± 47, εHf $_{(present)}$ = −2.5 ± 1.7; Penglai: n = 8, ^{176}Hf/^{177}Hf = 0.282872 ± 30, εHf $_{(present)}$ = +3.1 ± 1.0. All of these values are within error of the accepted values (Fisher et al., 2014a and sources cited above) and were also consistent with the long-term averages obtained using the same instrument. Results from the standards analyzed during this session are provided in Electronic Appendix B.

The values obtained for the Plešovice standard were used in monitoring instrumental drift. However, this standard was not used to apply analytical session-specific normalization factors (e.g. a final offset of the mass bias- and interference-corrected ^{176}Hf/^{177}Hf and ^{178}Hf/^{177}Hf of the unknowns) because this correction would only result in a one εHf $_{(present)}$ unit (at most) adjustment of the unknowns and due to the fact that the values for Plešovice remain consistent within and across the sessions.

In the summary table contained in Electronic Appendix 'A' and the full dataset contained in Electronic Appendix 'B', the quoted uncertainties are 2σ error of the mean for the ≤60 cycles. For the individual analyses, the initial ^{176}Hf/^{177}Hf values are corrected for ingrowth using the measured ^{176}Lu/^{177}Hf ratio. However, the uncertainty on the initial value only reflects uncertainty in the present-day ^{176}Hf/^{177}Hf value and does not account for error in the ^{176}Lu/^{177}Hf or age-related uncertainty. Due to the low ^{176}Lu/^{177}Hf exhibited by all of the zircons, however, this uncertainty should be almost negligible. In all of the tables and figures, εHf $_{(present)}$ is calculated using present-day CHUR values of ^{176}Hf/^{177}Hf = 0.282785 and ^{176}Lu/^{177}Hf = 0.0336 (Bouvier et al., 2008). For figures with the depleted mantle evolution line, present-day values of ^{176}Hf/^{177}Hf and ^{176}Lu/^{177}Hf of the depleted mantle are 0.283214 and 0.0399, respectively (Goodge and Vervoort, 2006).

4.4. Post-analysis cathodoluminescence (CL) imaging

CL images were acquired following the Hf and U–Pb analyses of the unpolished zircon grains. This theoretically enables each analytical volume to be examined a-priori in relation to the CL images (as opposed to relying on the assumption that each analytical volume remained within the same CL zone(s) identified on a polished zircon cross-section).

Following the U–Pb and Hf LA-ICP-MS analyses, a carefully chosen (described in Section 5) subset of zircon grains were removed from the initial mount and then re-mounted on double-sided tape with the LA-ICP-MS pits oriented parallel to the mounting surface. Following fixation in epoxy, the zircons were polished to expose the LA-ICP-MS pits in cross-section prior to the acquisition of Cl images using a JEOL JXA-8200 Superprobe housed in the Department of Earth and Planetary Sciences at Rutgers University. The instrument was operated at 15 kV and 5 nA with the CL signal collected on a JEOL Panchromatic CL Detector followed by processing using JEOL's xCLent X-ray and CL microanalyser.

5. Results

One hundred fifty seven U–Pb and 141 Hf isotope measurements on zircon resulted in useable data (Electronic Appendix 'A' and Electronic Appendix 'B'). The U–Pb ages are summarized on Fig. 3 and the Hf isotope results are shown on Fig. 4. In Fig. 2, a schematic cross-section illustrates the lithostratigraphic relations among the various groups of samples. Representative CL images of the post-analytical zircon cross-sections, in many cases showing the U–Pb and Hf analytical volumes, are provided in Fig. 5 (full size un-annotated images are presented in Electronic Appendix C).

Shown with the post analytical CL images in Fig. 5 are plots of the present-day Hf isotope composition, the raw ^{206}Pb/^{238}U, and the raw ^{207}Pb/^{206}Pb as a functions of depth within the Hf and U–Pb LA-ICP-MS analytical volumes. The Hf isotope depth profiles are constructed by averaging cycles in groups of 6 instead of averaging all of the cycles over the entire analytical volume (see Section 4.3). The U–Pb depth profiles are simply the raw ^{206}Pb/^{238}U and ^{207}Pb/^{206}Pb observed during each analysis.

5.1. Mesoproterozoic arc gneisses

The three gneiss samples from the NJH yielded an abundance of euhedral reddish-brown zircon grains up to 250 μm in width. Of the nine zircon U–Pb analyses from NAZ15-12, eight produced ^{206}Pb/^{238}U ages ranging from 1041.8 ± 8.5 to 959 ± 11 Ma (Fig. 3a) and one ^{206}Pb/^{238}U age of 743 ± 32 Ma (Fig. 3a). Five of the nine zircons were analyzed for Hf, resulting in calculated initial ε_{Hf} values ranging from −3.1 ± 1.2 to +5.6 ± 1.3 (Fig. 4a). However, if the results from the 743 ± 32 Ma aged zircon are excluded, the remaining zircons give a weighted mean ^{206}Pb/^{238}U age of 1004 ± 36 Ma and a weighted mean initial ε_{Hf} value of +3.8 ± 1.7.

Five U–Pb analyses from zircon in NAZ15-13 yielded a range of ^{206}Pb/^{238}U age from 1210 ± 110 to 906.4 ± 7.5 Ma (Fig. 3a), while the calculated initial ε_{Hf} values for these same zircons range from +6.8 ± 0.7 to +0.1 ± 0.7 (Fig. 4a). Again, if the results from the outlier at 1210 ± 110 Ma (Fig. 3a) are excluded, zircons in this sample yield a weighted mean ^{206}Pb/^{238}U age of 953 ± 60 Ma and a weighted mean initial ε_{Hf} value of +1.5 ± 1.7.

Ten U–Pb analyses were collected for NAZ15-14, resulting in ^{206}Pb/^{238}U ages ranging from 1053.7 ± 7.1 to 824.1 ± 4.7 (Fig. 3a). The corresponding calculated initial ε_{Hf} values range from +0.9 ± 1.0 to −3.3 ± 0.8 (Fig. 4a). If the results from the 824 ± 4.7 Ma outlier among these data are excluded, zircons in this sample give a weighted mean ^{206}Pb/^{238}U age of 1012 ± 30 Ma and a weighted mean initial ε_{Hf} value of 0.15 ± 0.86.

The CL images of the post-analytical zircon cross-sections from the gneiss samples (upper row of Fig. 5) display a variety of textures. Most are consistent with simple magmatic growth resulting in concentric oscillatory and sector zoned zircon crystals, but some zircons display convolute and patchy textures that are consistent with

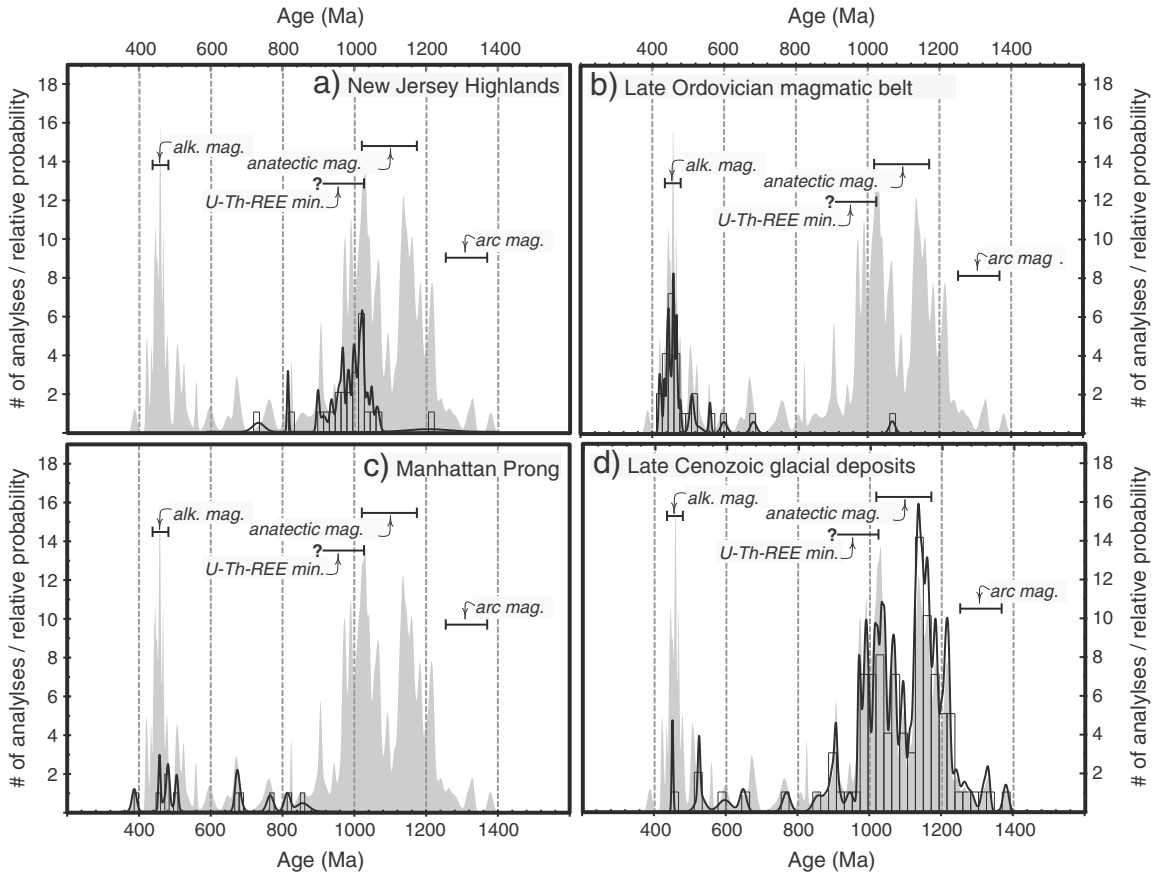

Fig. 3. Probability density curves calculated using Isoplot 3.7 (Ludwig, 2012) and histograms (bin size = 50) constructed using the individual $^{206P}b/^{238}U$ apparent ages for the zircons analyzed in this study. Plots are organized according to the lithostratigraphic subdivisions (see Fig. 2). The gray shaded region on the plots represents a probability density curve that was calculated using all of the $^{206P}b/^{238}U$ ages determined in this study. The age-ranges of major tectonic and magmatic events that affected the Laurentian margin are also shown on the individual panels in the figure.

metamorphic recrystallization (Corfu et al., 2003). None of the zircons for which CL images are available display conspicuous evidence of containing xenocrystic (i.e., inherited) domains, but a few images show internal complexity that could indicate multi-stage growth.

Several of the zircons are also characterized by rim domains that appear brighter in CL when compared to the oscillatory and/or sector zoned interior domains (NAZ15-12-1, NAZ15-14-3, NAZ14-14-1, and NAZ15-14-6). However, examination of the Hf and U–Pb depth profile data from these zircons (Fig. 5a) does not indicate the existence of a dramatic shift in the U–Pb or Hf isotope systematics across the boundary between the bright CL domains and the interior portions of the grains. Two of the U–Pb analyses (NAZ15-12-1 and NAZ15-14-3) are characterized by changes in the behavior of the raw $^{206}Pb/^{238}U$ values towards the bottom of the analytical volume, and this is reflected in the higher 2σ uncertainty in their $^{206}Pb/^{238}U$ ages.

5.2. Cortlandt-Beemerville magmatic belt

Ten U–Pb analyses from the Bedford Complex augen gneiss (NAZ15-04) gave $^{206}Pb/^{238}U$ ages from 423.7 ± 5.4 to 523 ± 28 (Fig. 3b). Only five Hf analyses were obtained from this sample, giving calculated initial ε_{Hf} values from −2.5 ± 1.1 to −1.3 ± 1.2 (Fig. 4b). The weighted mean $^{206}Pb/^{238}U$ age of the five zircons is 454 ± 17 Ma and that of the initial ε_{Hf} value is −1.85 ± 0.46 (Fig. 4b). For the Bedford Complex monzonite (NAZ15-05), five U–Pb analyses yielded $^{206}Pb/^{238}U$ ages from 509.8 ± 9.8 to 419.5 ± 4.5 Ma (Fig. 3b). These same zircons also produced calculated initial ε_{Hf} values from +2.4 ± 1.6 to +1.2 ± 1.0 (Fig. 4b). The weighted mean $^{206}Pb/^{238}U$ age and initial ε_{Hf} value are 449 ± 32 Ma and 1.74 ± 0.39, respectively.

Five U–Pb analyses were collected from the Peach Lake Complex monzodiorite (NAZ15-07), resulting in $^{206}Pb/^{238}U$ ages from 1059 ± 16 to 451.1 ± 5.7 (Fig. 3b). Hf analyses of these same five of the zircons gave four calculated initial ε_{Hf} values from −0.2 ± 1.7 to −2.2 ± 1.2 and one outlier value of +10.0 ± 1.7.

The nepheline syenite from the Beemerville Complex (NAZ15-10) only yielded enough zircon to obtain data on five different grains. They yielded $^{206}Pb/^{238}U$ ages from 507 ± 12 to 441 ± 25 Ma (Fig. 3b), calculated initial ε_{Hf} values from −0.9 ± 2.4 to +0.4 ± 2.8 (Fig. 4b), and weighted mean $^{206}Pb/^{238}U$ age and initial ε_{Hf} value of 465 ± 13 Ma and +0.28 ± 0.50, respectively.

As for the CL images of the post-analytical zircon cross-sections (Fig. 5b), two of the zircons from NAZ15-04 display simple oscillatory zoning, whereas a third zircon displays a convoluted and patchy pattern. One of the zircons from NAZ15-07 displays a CL pattern consistent with the existence of a xenocrystic oscillatory zoned core overgrown by a younger rim that is dark and homogeneous in CL, whereas the other zircon exhibits a homogeneous and dark core surrounded by a weakly zoned and lighter rim. The single zircon imaged in CL from NAZ15-10 displays weak patchy zoning.

Examination of the Hf and U–Pb depth profiles of zircons NAZ15-04, NAZ15-05, and NAZ15-10 (Fig. 5b) indicates that the grains are relatively homogeneous in their U–Pb and Hf isotope compositions within the sampled analytical volumes. However, both analyses from sample NAZ15-07 display dramatic shifts in the Hf and U–Pb compositions as a function of depth. In the both analyses, these shifts can be correlated

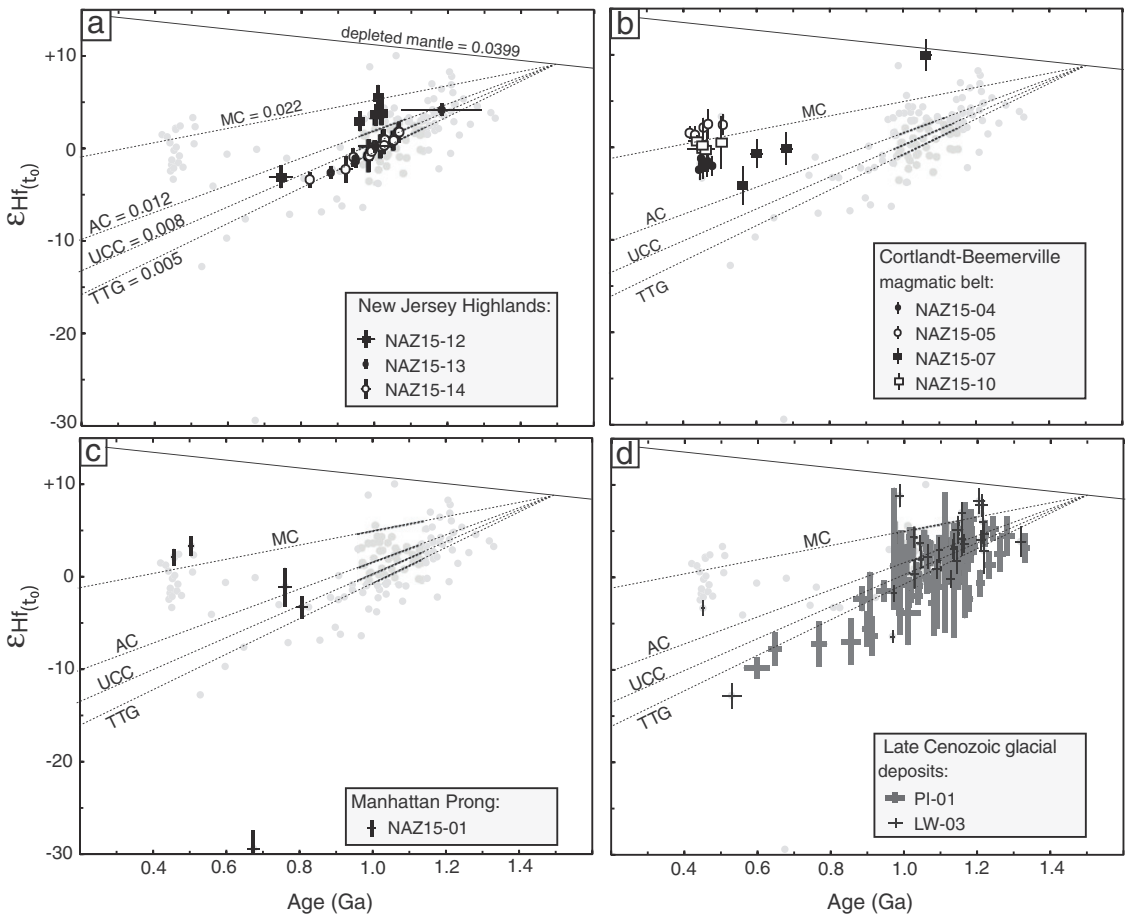

Fig. 4. Plots of zircon ingrowth-corrected ε_{Hf} values against their $^{206}Pb/^{238}U$ apparent ages. (a) Mesoproterozoic magmatic arc rocks in the New Jersey Highlands; (b) Late Ordovician alkaline magmas in the Cortlandt-Beemerville magmatic belt; (c) Manhattan Prong; and (d) Late Cenozoic glacial deposits. Separate symbols are used for each sample, with bar height and width corresponding to the 2σ uncertainties in ε_{Hf} values and $^{206}Pb/^{238}U$ ages. The data from the individual samples are superimposed on gray dots denoting the $\varepsilon_{Hf(initial)}$ of all the analyses. The Hf isotope evolution line for the depleted mantle was calculated using present-day values of $^{176}Hf/^{177}Hf$ and $^{176}Lu/^{177}Hf$ of 0.283214 and 0.0399 (Goodge and Vervoort, 2006), respectively. The crustal evolution lines were constructed using $^{176}Lu/^{177}Hf$ of 0.005 (the tonalite-trondhjemite-granite (TTG) reservoir of Blichert-Toft and Albarède, 2008), 0.008 (the average upper continental crustal (UC) reservoir of Rudnick and Gao, 2003), 0.012 (the arc crustal (AC) reservoir of Rudnick and Gao, 2003), and 0.022 (the mafic crustal (MC) (source of Amelin et al., 1999). All lines were calculated from an $\varepsilon_{Hf} = 8.9$ starting value at 1.5 Ga).

with the location of the xenocrystic cores observed in the corresponding CL images.

5.3. Manhattan Prong schist

The single sample from the Manhattan Prong (NAZ15-01) yielded only a small amount of zircon with typical grain sizes of <15 μm. Nonetheless, ten zircons of a size sufficient for at least one U–Pb measurement were found. Ten U–Pb analyses gave $^{206}Pb/^{238}U$ ages from 849 ± 35 to 387 ± 13 Ma (Fig. 3c). Only five Hf analyses could be performed, resulting in calculated initial ε_{Hf} values from +2.1 ± 0.9 to −29.5 ± 2.0 (Fig. 4c).

Only one post analytical CL image could be obtained from this sample due to the small size of the zircons (Fig. 5, last row). Both the U–Pb and Hf analytical volumes are visible in the image. It is evident that this zircon is characterized by convolute and patch internal zoning, but there does not appear to be any evidence of a xenocrystic domain. The depth-dependent Hf and U–Pb isotopic systematics from this analysis (NAZ15-01-09; Fig. 5e) indicate that, while the Hf isotope composition remains relatively homogeneous within the Hf analytical volume, there is some complex behavior in the raw $^{206}Pb/^{238}U$ observed as a function of depth within the U–Pb analytical volume.

5.4. Glacial tillite samples

Thirty U–Pb analyses were collected from sample LW-03, producing $^{206}Pb/^{238}U$ ages ranging from 1214.2 ± 9.9 to 450.1 ± 4.4 (Fig. 3d). Hf analyses were performed for twenty-seven of the thirty grains analyzed for U–Pb, resulting in calculated initial ε_{Hf} values ranging from −12.8 ± 1.4 to +8.2 ± 1.4 (Fig. 4d).

Seventy U–Pb analyses were collected from sample PI-01 (described in Section 2.2.4), yielding $^{206}Pb/^{238}U$ ages ranging from 1330 ± 11 to 647 ± 18 (Fig. 3d). Hf analyses were performed for sixty-nine of the seventy grains that were analyzed for U–Pb, resulting in calculated initial ε_{Hf} values of −9.8 ± 1.2 to +6.4 ± 1.0 (Fig. 4d).

The CL images of the post-analytical zircon cross-sections from the glacial tillites (Fig. 5c and d) display a range of textures. Some are similar to those observed in the Mesoproterozoic arc crustal basement and Late Ordovician alkaline magmas; others display textures not seen in any of the basement rock samples but their patterns are still consistent with magmatic growth. Some of the zircons in the tillite samples also display the bright CL rim domains observed in the NJH basement zircons. Examination of the Hf and U–Pb depth profile data from the zircons in sample LW-03 (Fig. 5c) suggests that there may be a subtle change in the behavior of the raw $^{206}Pb/^{238}U$ associated with the transition from bright CL

rim to the oscillatory zoned interior domain (e.g. analysis LW03-05), whereas the Hf isotope composition remains relatively homogeneous throughout.

The observations are similar for the depth profile data from sample PI-01 (Fig. 5d); with the exception that one zircon (analysis PI-01-65) displays evidence for complex behavior in the observed $^{206}Pb/^{238}U$ profile. While Hf does not suggest a drastic shift in Hf isotope composition, the CL image from this zircon is indicative of a complex growth and/or alteration history, possibly involving disturbance(s) to the zircon's structure (e.g. Corfu et al., 2003).

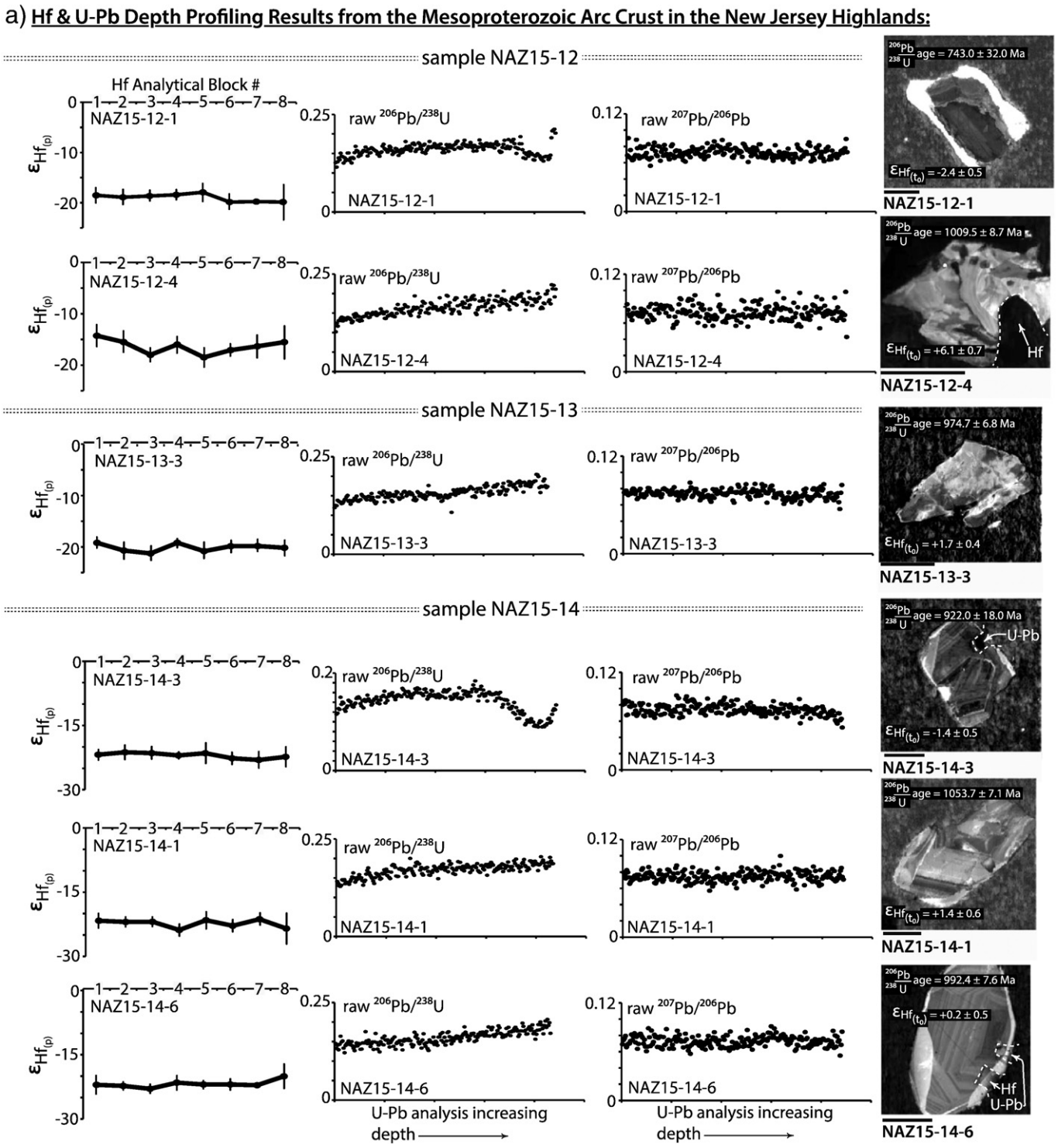

Fig. 5. a–e: Post-analytical zircon cathodoluminescence (CL) images accompanied by plots of the present-day Hf isotope composition, raw $^{206}Pb/^{238}U$, and raw $^{207}Pb/^{206}Pb$ as a function of depth. Higher quality, un-annotated versions of these CL images are provided in Electronic Appendix C. Note that the labels for the individual depth profiles and CL images correspond with the labeling in supplementary Table 1. The results are organized into panels (a–e) according to the major lithostratigraphic delineations. The exception is that the results from each of the glacial tillite samples are shown separately: a) Mesoproterozoic arc crust in the New Jersey Highlands; b) Late Ordovician alkaline magmas; c) Late Wisconsinan tillite sample LW-03; d) Pre-Illinoian tillite sample PI-01; and e) Manhattan Prong.

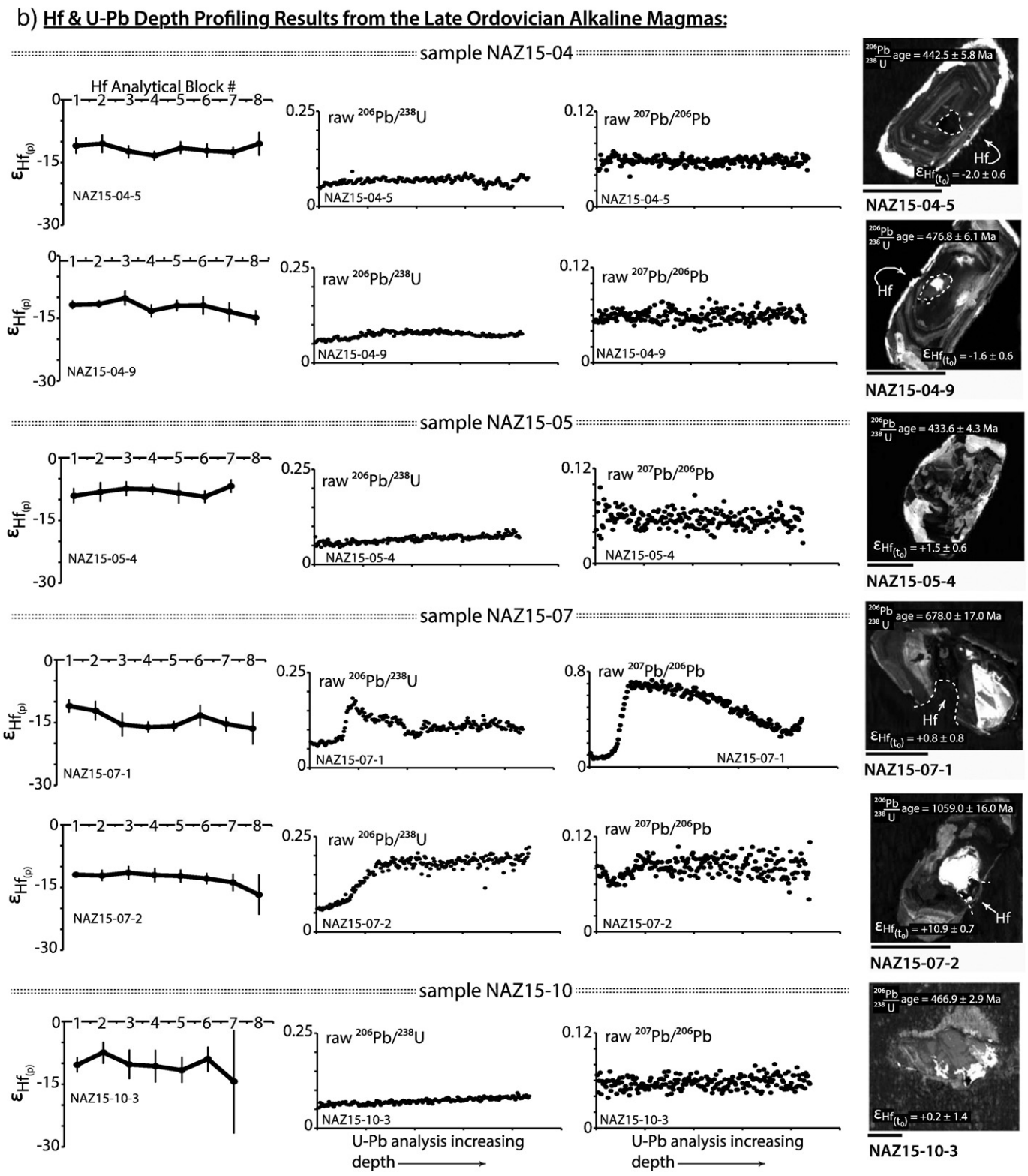

Fig. 5 (*continued*).

6. Discussion

6.1. The Hf isotope record of continental margin arc and anatectic magmatism

Laurentian continental margin arc magmatic activity in the NJH has previously been constrained to date from 1366 ± 9 Ma to 1248 ± 12 Ma (Volkert et al., 2010). This range includes the rocks of the Losee suite. A basic observation of the present data (see summary table in Appendix A and Fig. 3a) is that most of the $^{206}Pb/^{238}U$ ages from the NJH rock samples cluster around ~1.0 Ga (Fig. 3a), with only a single zircon grain yielding a poorly constrained ~1.2 Ga age and two grains defining ages of ~0.8 Ga or younger. The range defined by the zircons in the

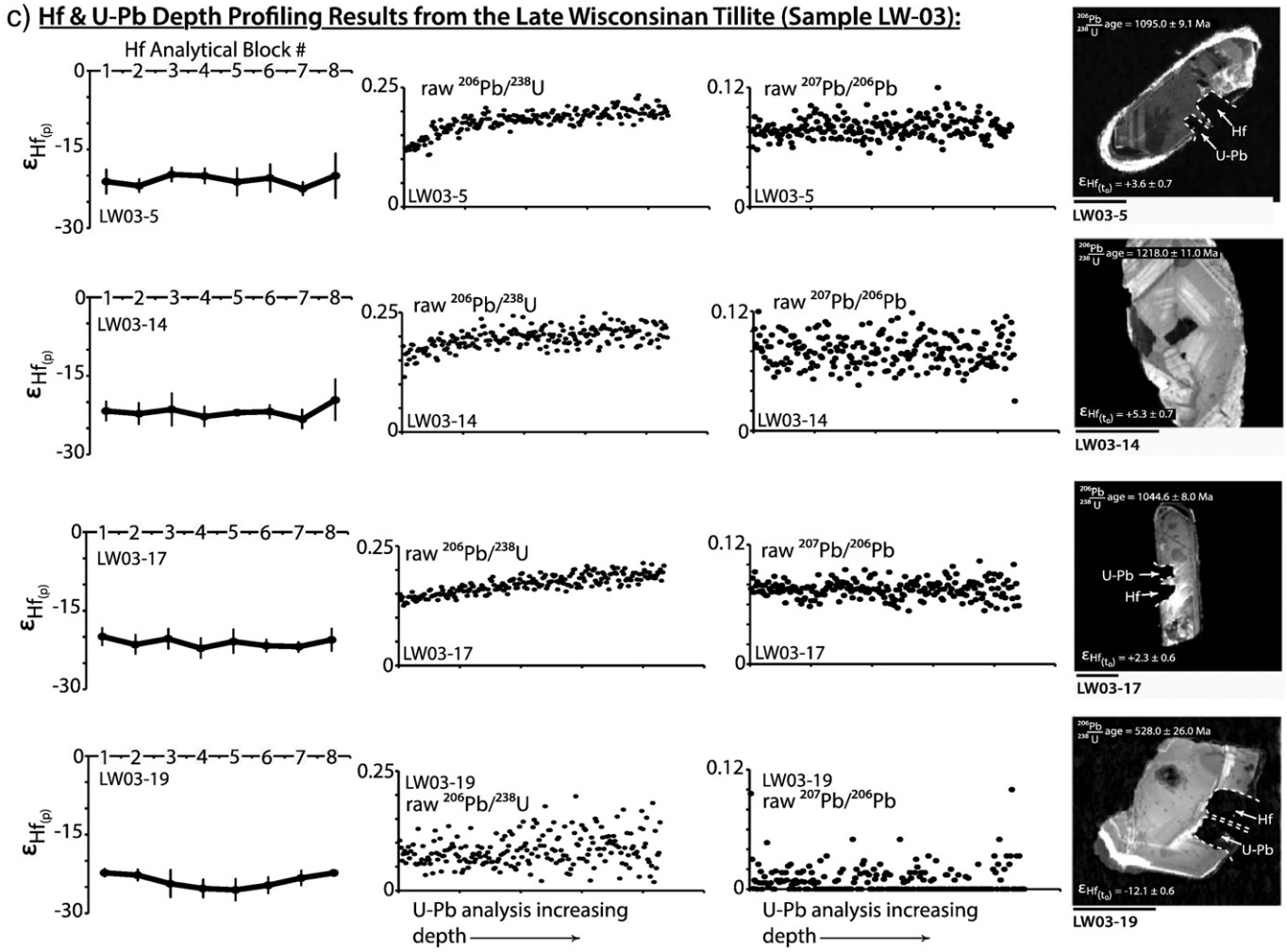

Fig. 5 (*continued*).

NJH rock samples overlaps (Fig. 3a) the timing of Mesoproterozoic anatectic magmatism that occurred throughout the NJH between 1188 ± 6 and 1019 ± 4 Ma (Volkert et al., 2010), but it does not encompass the timing of continental margin arc magmatic activity that occurred from ~1.4 Ga to ~1.2 Ga. The age range from the NJH samples also extends into the period where hydrothermal, metamorphic, and magmatic activities have affected the NJH (Volkert et al., 2010).

In contrast, the two glacial tillite samples (PI-01 and LW-03) both contain a small number of zircons with ages that fall within the time period of continental margin arc magmatism (>1.2 Ga; Fig. 3d). This means that it should be possible to combine them with the NJH rock-sample data for the purpose of understanding the Hf isotope records of continental margin arc magmatism and subsequent anatectic magmatism.

Examination of Fig. 4d reveals that all of the zircons from the glacial tillite samples with ages between ~1.2 Ga and ~1.4 Ga have positive $\varepsilon_{Hf(initial)}$ values. The occurrence of only positive $\varepsilon_{Hf(initial)}$ values before ~1.2 Ga suggests that the Laurentian margin arc crust originated as juvenile material produced by partial melting of the depleted upper mantle. Comparison of Fig. 4d and Fig. 4a reveals, however, that the positive $\varepsilon_{Hf(initial)}$ values older than 1.2 Ga define the more radiogenic end of an array that progresses towards more unradiogenic values. This progression is especially pronounced in the NJH rock samples (Fig. 4a), but it can also be observed in the tillite (Fig. 4d) dataset. However, it is necessary to consider whether this progression actually represent a crustal evolution trend, or if it is artificial before the data can be used to understand the Laurentian margin.

6.1.1. Is the Laurentian margin crustal evolution array real?

It is well-recognized that underestimation of the zircon crystallization age for the calculation of $\varepsilon_{Hf(initial)}$ values will result in $\varepsilon_{Hf(initial)}$ values that are artificially low (e.g., Guitreau and Blichert-Toft, 2014Kemp et al., 2009). This underestimation can result from inadvertently combining the U–Pb age and Hf isotope composition for zircon sub-domains with different ages, or from disturbances of the U–Pb system. This is a potential problem for the present study because, while only zircons in one sample (NAZ15-07) were found to display CL evidence of xenocrystic cores (Fig. 5b), only a subset of the zircons analyzed for U–Pb and Hf were imaged in CL. This means that this issue of the potential for the Hf analytical volume to have fallen within a different domain than the U–Pb analysis needs to be considered further.

Guitreau and Blichert-Toft (2014) advocate that the only way to mitigate the potential for inadvertently combining domains of different ages is by the split-stream technique wherein the U–Pb age and Hf isotope systematics are measured for the same analytical volume (e.g. Fisher et al., 2014b). This is partly because the use of CL images collected from polished zircon cross-sections does not necessarily provide information about the relationship of separate Hf and U–Pb analytical volumes at depth in a zircon crystal. However, the instrumentation needed to perform the split-stream measurement is not yet everywhere

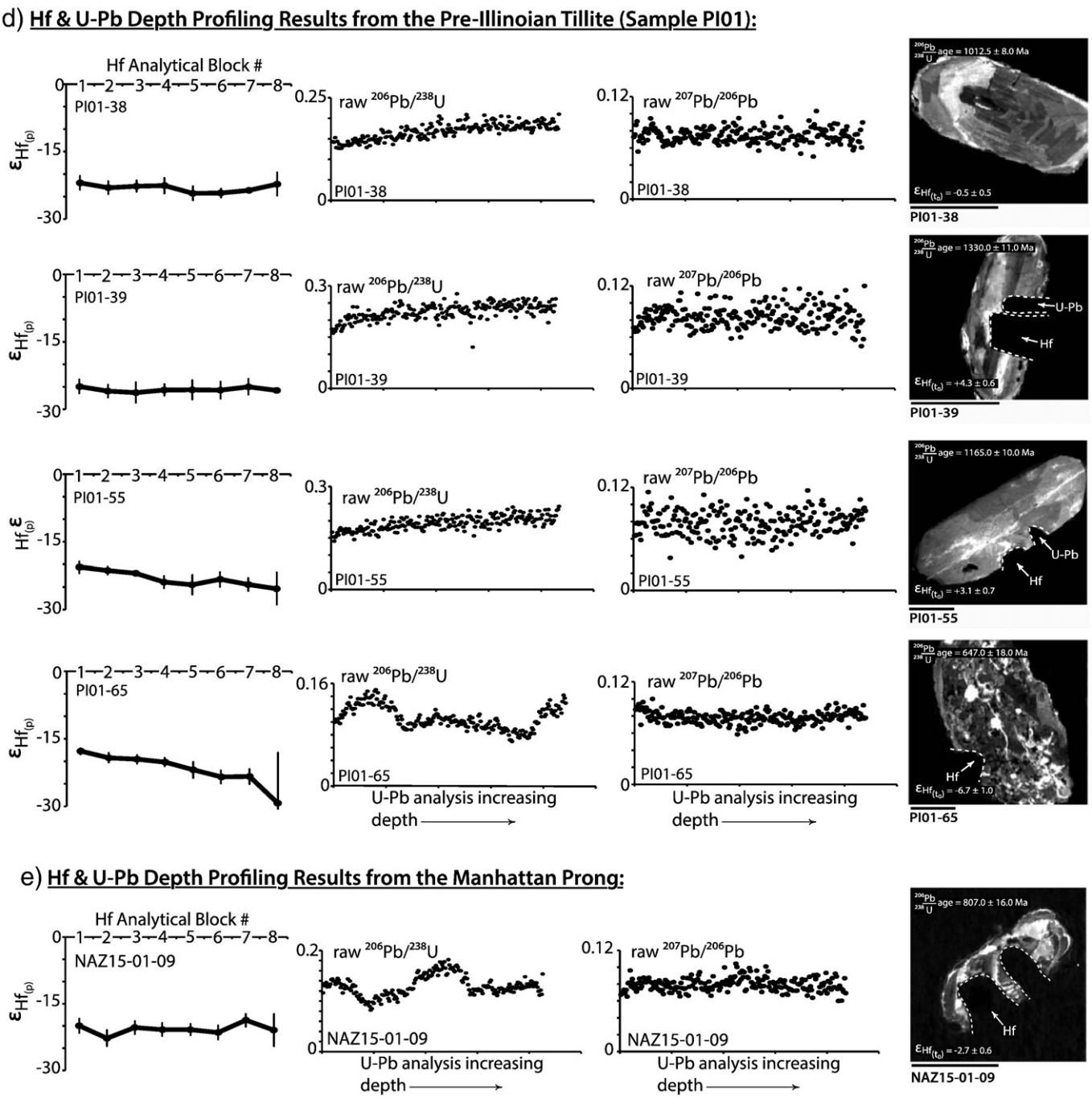

Fig. 5 (*continued*).

available. Therefore, while it is necessary to factor this source of uncertainty into any interpretations derived from the crustal evolution arrays, the generally internally consistent nature of the zircon U–Pb ages from each of the samples suggests that there is not a systematic error in the choice of age for the calculation of the $\varepsilon_{Hf(initial)}$ values in this study.

For some of the zircons in this study, it is possible to directly evaluate the relationships between the U–Pb and Hf isotope analytical volumes (Fig. 5). Due to the well-recognized depth dependent inter-element fractionation that occurs during LA-ICP-MS U–Pb zircon analyses (especially when performed on a single collector instrument), the final $^{206}Pb/^{238}U$ value is determined by projection through the individual cycles of data back to an initial value. In contrast, very little depth dependent fractionation exists for the $^{207}Pb/^{206}Pb$ (e.g. Gehrels et al., 2008). It is therefore difficult to relate changes in the raw $^{206}Pb/^{238}U$ observed during individual analyses to actual changes in the $^{206}Pb/^{238}U$ age.

However, it is reasonable to assume that abrupt shifts in the raw $^{206}Pb/^{238}U$, especially where these shifts are also accompanied by changes in the raw $^{207}Pb/^{206}Pb$, could indicate U–Pb age heterogeneity within the analytical volume. For the Hf isotope analyses, which are performed on a multi-collector, the depth dependent fractionation is much less severe than for the U–Pb system. The result is that changes in the observed ε_{Hf} values as a function of depth within the analytical volume can be interpreted as real isotopic variation. In the case of the analytical conditions in this study, which are identical to those in Zirakparvar (2015), variations greater than 5 present-day ε_{Hf} units between the mean ε_{Hf} of the individual groups of 6 cycles from each Hf analysis can

reasonably be interpreted as actual variations in the Hf isotope composition.

With these considerations in mind, examination of the Hf and U–Pb depth profiling results from the individual samples (Fig. 5a–e) indicates that only the zircons from one sample (NAZ15-07) contain core and rim domains that obviously exhibit different U–Pb ages and drastically different Hf isotope compositions. While some of the zircons from the other samples do exhibit minor complexity in their U–Pb and Hf isotope systematics, which is sometimes associated with the occurrence of very bright CL rims and/or complex zoning characteristics, none of their zircons exhibit drastic changes in the behavior of the U–Pb and Hf isotopes within their respective analytical volumes. It should be noted that these depth profiling considerations were applied to each analysis, but that only the analyses for which CL images were also obtained are shown in Fig. 5. This further suggests that the $\varepsilon_{Hf(initial)}$ values are calculated at the proper U–Pb age.

There are a variety of approaches (see discussion by Spencer et al. (2016)) to recognize spurious U–Pb ages that result from disturbances to the zircon's U–Pb systematics (e.g. Pb loss). However, there is no uniform filter that is applicable to every dataset, and as showed by Kemp et al. (2010) for certain Hadean zircons, the application of very rigorous criteria (e.g. Nemchin et al., 2006) can result in the exclusion of valid $\varepsilon_{Hf(initial)}$ values. In returning to the data from the Laurentian margin, it is important to consider that the younger portions (e.g. <800 Ma) of the crustal evolution array in question are partly defined by the 'outlier' zircons described in the results section from the NJH rock samples (Fig. 4a) and some of the more discordant zircons from the tillite samples. However, there is not a systematic relationship between the degree of discordance and either the $^{206}Pb/^{238}U$ ages or initial $\varepsilon_{Hf(initial)}$ values in either the NJH samples or the tillites (refer to full analytical dataset in Electronic Appendix 'A') that warrants establishing a lower-limit age cutoff for consideration of the $\varepsilon_{Hf(initial)}$ values.

Furthermore and as noted in the results section, removal of the 'outlier' analyses for the three NJH samples results in weighted mean $^{206}Pb/^{238}U$ ages that are all within-error of 1.0 Ga and sample average $\varepsilon_{Hf(initial)}$ values ranging from 0.15 ± 0.86 to 3.8 ± 1.7. These sample-average values are unradiogenic relative to the majority of the zircons with $^{206}Pb/^{238}U$ ages > 1.0 Ga in the glacial tillite samples (Fig. 4). Therefore, eliminating the 'outlier' zircons does not change the basic observation that the period of arc magmatism from 1.4 to 1.2 Ga produced magmas with more radiogenic Hf isotope compositions than those produced by anatectic melting of the arc crust between 1.2 and 1.0 Ga (Fig. 4). In total, these observations suggest that the crustal evolution array is real.

6.1.2. Hf isotope evolution of the Mesoproterozoic arc crust

On Fig. 4a and d, a series of crustal evolution lines have been drawn for different $^{176}Lu/^{177}Hf$ from a depleted-mantle like ($\varepsilon_{Hf} = +8.9$) starting composition at 1.5 Ga. While arc magmatism began at ~1.4 Ga (e.g. Volkert, 2012) and the oldest zircons documented in this study are ~1.4 Ga (Fig. 3), the 1.5 Ga starting point was selected to account for the likelihood that the arc-magmatism took place in lithosphere that was produced by partial melting of the depleted mantle before the onset of arc magmatism at ~1.4 Ga. Examination of Fig. 4a and d demonstrates that the majority of the zircons with ages between 1.4 and 0.8 Ga lie within an envelope defined by $^{176}Lu/^{177}Hf$ between 0.022 (the re-worked mafic crustal (MC) source of Amelin et al. (1999)) and 0.005 (the tonalite-trondhjemite-granite (TTG) reservoir of Blichert-Toft and Albarède (2008)).

This envelope encompasses evolution lines with $^{176}Lu/^{177}Hf$ of 0.012 and 0.008, the bulk upper continental crust (UCC) and bulk andesitic upper crust {AC), respectively, of Rudnick and Gao (2003); the former is similar to the value for juvenile upper crust suggested by Vervoort and Blichert-Toft (1999). Furthermore, only minor adjustments to the 1.5 Ga starting point or the $^{176}Lu/^{177}Hf$ ratios of the evolution lines would result in nearly *all* of the 1.4 to 0.8 Ga aged zircons lying within the envelope. These results clearly indicate that the Laurentian margin's Mesoproterozoic arc crust was derived from the depleted mantle reservoir. They also demonstrate that the post-arc anatectic magmas were produced primarily by re-working of the juvenile continental margin arc crust with only minor input of material from the depleted mantle reservoir.

However, it should be noted that there is a pulse of somewhat more radiogenic $\varepsilon_{Hf(initial)}$ values that occurs between ~1.1 Ga and 1.0 Ga (Fig. 4). This is during the margin's anatectic phase, and it is generally well understood that crustal anatexis in inactive continental arc and post-collision settings can be driven by melting in the mantle (Asmerom et al., 1991; Li et al., 2012, 2014; Solgadi et al., 2007). Slab-breakoff from beneath (e.g. Li et al., 2014), and/or delamination of an eclogitized residue from the base of (e.g. Solgadi et al., 2007), the continental margin lithosphere can allow for aesthenospheric influx. This can lead to melting of subduction-enriched lithospheric mantle as well as in the emplacement of partial melts derived directly from the upwelled aesthenosphere into the lithosphere.

The pulse of more radiogenic values that occurs between ~1.0 Ga and ~1.1 Ga (Fig. 4) is most consistent with melting of subduction enriched lithospheric mantle. This is because most of the more radiogenic $\varepsilon_{Hf(initial)}$ values between ~1.1 Ga and ~1.0 Ga cluster at or beneath the mafic crustal evolution line ($^{176}Lu/^{177}Hf = 0.022$; Amelin et al., 1999) as it evolves from a depleted mantle-like starting Hf isotope composition at ~1.5 Ga. The two analyses with U–Pb ages between ~1.1 and ~1.0 Ga that are characterized by $\varepsilon_{Hf(initial)}$ values approaching the depleted mantle Hf isotope composition may also signify that aesthenospheric melts interacted with the Laurentian margin crust during the anatectic phase. However, additional data is needed to further explore this possibility.

6.2. Evolution of the lithospheric mantle beneath the Laurentian continental margin

The bulk compositions (Ratcliffe, 1981) of the magma bodies comprising the Late Ordovician aged magmatic belt, and their relationship to the Mesoproterozoic basement they intrude, indicate that they are not anatectic melts of the crust. There is also no evidence that arc magmatism leading up to the Taconic orogeny affected the study area-instead, there is only weakly preserved deformation associated with this event (Ratcliffe, 1981). In contrast, Laurentian margin rocks to the northeast and southwest of the study area preserve a record of intense deformation during the Taconic orogeny. These observations have led researchers to conclude that the Late Ordovician magmatic belt was intruded as a result of a lithospheric-scale instability created by differences in the timing of tectonic collisions in the north and south of the study area (e.g. Ratcliffe, 1981).

Most of the intrusions in the Late Ordovician magmatic belt have bulk compositions suggesting that their parent magmas were produced by melting of the lithospheric mantle beneath the Mesoproterozoic arc crust (Ratcliffe, 1981) and therefore provide an opportunity to study its evolution as a function of the region's tectonic history. Examination of the U–Pb ages (Fig. 3b) reveals that the three samples from the Bedford and Beemerville complexes (NAZ15-04, NAZ15-05, and NAZ15-10) yield weighted-mean U–Pb ages that are within error of each other and consistent with the most recently published high-precision U–Pb geochronological data for the belt (Ratcliffe et al., 2012). In contrast, U–Pb ages from the Peach Lake Complex (sample NAZ15-07) span a wide range back to ~1.1 Ga (Fig. 2b), suggesting that the latter zircons were inherited from the country rocks. This is not surprising given that the sample from the Peach Lake Complex is the least primitive bulk composition of all the Late Ordovician magmatic rock samples examined in this study. Therefore, we use only the Bedford and Beemerville complex samples to understand the nature of the lithospheric mantle.

The nepheline syenite from the far western end of the magmatic belt (NAZ15-10) is the most primitive bulk composition available for study. Because the nepheline syenite body is associated with kimberlitic dikes (Eby, 2004), it is likely that its Hf isotopic composition most closely reflect that of the lithospheric mantle. The weighted mean initial ε_{Hf} value of 0.28 ± 0.50 from sample NAZ15-10 is within-error of that of the CHUR reservoir. Because the depleted upper mantle at ~0.5 Ga would have had an ε_{Hf} of ~+13 (assuming a present-day $^{176}Lu/^{177}Hf$ of 0.0399), there are two possible explanations for the nearly chondritic ε_{Hf} value of the nepheline syenite. One is that the sample crystallized from a melt that was related to the arrival of a plume sourced from a chondritic reservoir in the deep mantle; the other is that the lithospheric mantle evolved to this composition as a consequence of the region's tectonic history. The latter possibility is implicated because there is no evidence of a Late Ordovician plume-related large igneous province anywhere in the vicinity of the study area.

Examination of the results from the Proterozoic aged zircons (Fig. 4a and d) in the tillites suggests that the region was underlain by a mantle capable of producing radiogenic ε_{Hf} values during the time of continental margin arc magmatic activity between ~1.4 and ~1.2 Ga. In order to evolve to an ε_{Hf} that intersects the $\varepsilon_{Hf(initial)}$ values from the Late Ordovician magmas, a reservoir with a depleted mantle-like Hf isotope composition prior to the start of arc magmatism at ~1.4 Ga (i.e., with an $\varepsilon_{Hf} = 8.9$, at 1.5 Ga) could have had a $^{176}Lu/^{177}Hf$ of ~0.022.

This value is significantly higher than the crustal evolution arrays that satisfy most of the Mesoproterozoic arc crust zircons ($^{176}Lu/^{177}Hf = 0.012–0.005$), but it is still lower than the $^{176}Lu/^{177}Hf$ of the depleted mantle or CHUR reservoirs. Given the history of subduction beneath the continental margin during the Mesoproterozoic (Volkert et al., 2010), it is possible that portions of the mantle wedge beneath the margin were contaminated by Hf from subducted continental crustal material. The $^{176}Lu/^{177}Hf$ of 0.022 is also consistent with what would be expected for an overall mafic to ultramafic reservoir capable of producing magmas with relatively primitive bulk compositions (e.g. Amelin et al., 1999; Kemp et al., 2010).

Another relevant observation is that the sample-average ε_{Hf} values of the eastern end of the Late Ordovician magmatic belt (NAZ15-04 with an $\varepsilon_{Hf(initial)}$ of −1.85 ± 0.46 and NAZ15-05 with an $\varepsilon_{Hf(initial)}$ of 1.74 ± 0.39) are nearly the same as that from the nepheline syenite (above). The exception is the monzodiorite sample from the Peach Lake Complex (sample NAZ15-07), which as discussed above, apparently contains inherited zircons suggesting it was produced by melting of the regional crust. This suggests that the contaminated lithospheric mantle with a $^{176}Lu/^{177}Hf$ ratio of ~0.02 was a relatively widespread feature of the region. The small differences in $\varepsilon_{Hf(initial)}$ among the Ordovician magmatic samples could have resulted from slightly varying extents of contamination and other subtle factors. However, the data clearly provides evidence for the presence of subduction enriched lithospheric mantle beneath the continental margin.

6.3. Preliminary assessment of the tectonic provenance of metasediments in the Manhattan Prong

The provenance and tectonic history of the metamorphic rocks in the Manhattan Prong have been the subject of a number of studies (e.g. Long and Kulp, 1958; Merguerian, 1983; Mose and Hayes, 1975; Mose et al., 1975; Paige, 1955; Prucha, 1956). The 10 zircon U–Pb ages from the Manhattan Schist, which is inferred to have a sedimentary protolith, span a range of ages from ~0.9 Ga to ~0.4 Ga (Fig. 3c), and most of the $\varepsilon_{Hf(initial)}$ values are broadly consistent with derivation of zircons from the Laurentian margin (Fig. 4). One $\varepsilon_{Hf(initial)}$ value from a ~ 700 Ma zircon is much lower, at −29.5 ± 2.0. While there is only a limited dataset available from the Manhattan Schist, it is still possible to speculate about the meaning of this single highly unradiogenic value.

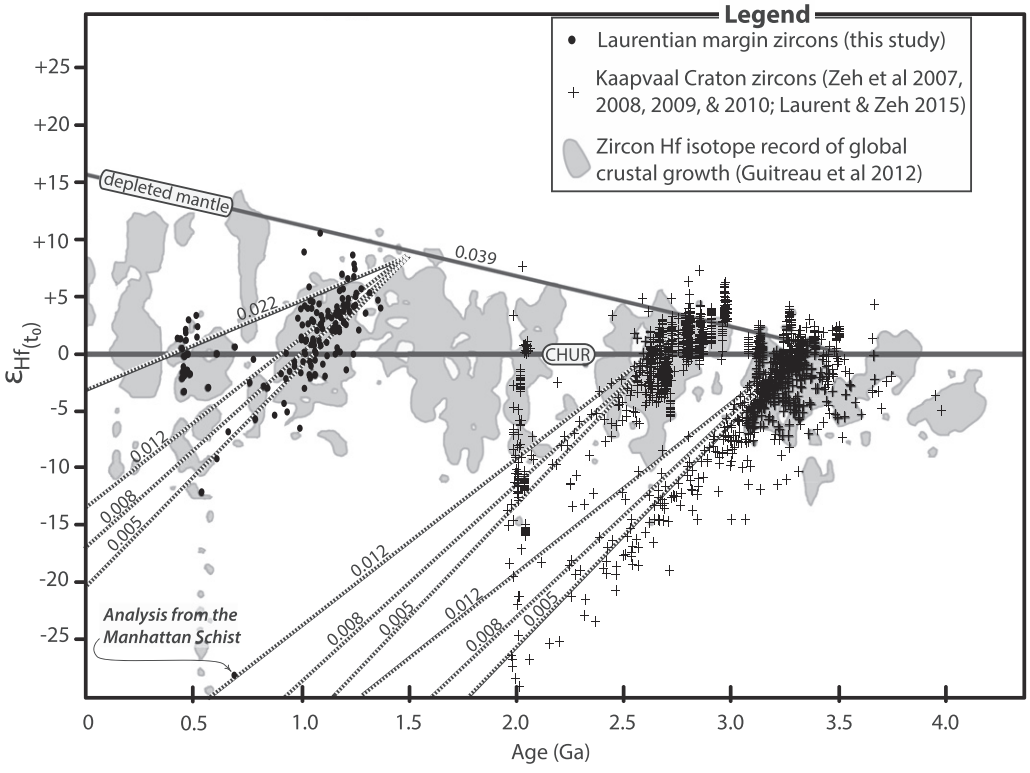

Fig. 6. Plot of the ingrowth-corrected $\varepsilon_{Hf(initial)}$ values from the Laurentian margin (circles) as well as a compilation of $\varepsilon_{Hf(initial)}$ values from the tectonic boundary zone between the Kaapvaal and Zimbabwe cratons in southern Africa (triangles). Kaapvaal and Zimbabwe data are from Zeh et al. (2007, 2008, 2009, 2010) and Laurent and Zeh (2015). Uncertainty associated with the individual ε_{Hf} values is not shown to maintain clarity. Both data sets are superimposed on gray fields representing the global detrital zircon record of continental growth (adapted from Guitreau et al., 2012). The sources of the values used in constructing the depleted mantle and crustal evolution lines are provided in the caption of Fig. 4.

On Fig. 6, it can be seen that the single highly unradiogenic ε_{Hf} value from the Manhattan Schist plots close to a prominent excursion towards highly unradiogenic values in the global zircon Hf isotope crustal growth record. The zircons defining these excursions are interpreted as reflecting the re-working of Archean crust (Guitreau et al., 2012). On Fig. 6, the $\varepsilon_{Hf(initial)}$ values from the Laurentian margin samples are also shown with $\varepsilon_{Hf(initial)}$ values from the broad tectonic boundary zone between the Kaapvaal and Zimbabwe cratons in southern Africa. The latter are compiled from Zeh et al. (2007, 2008, 2009, 2010) and Laurent and Zeh (2015).

The Kaapvaal–Zimbabwe values are from a wide variety of rock types recording a protracted history of continental margin-arc and oceanic island-arc magmatism that began with the production of mafic crust in an intra-oceanic environment at ~3.4 Ga (Laurent and Zeh, 2015) and was followed by episodic continental margin arc magmatism and non-arc related magmatism until ~2.6 Ga (see summary figure 13 in Zeh et al. (2009)) when the two cratons were sutured together. The Kaapvaal-Zimbabwe dataset also encompasses a major pulse of post-orogenic magmatism (the Bushveld event at ~2.06 Ga) that affected the tectonic boundary zone ~600 m.y. following the end of the last arc-magmatic event. Interestingly, a Hf isotope crustal evolution line corresponding to $^{176}Lu/^{177}Hf = 0.012$ plotted through the Kaapvaal-Zimbabwe data set beginning with a depleted-mantle like composition at ~2.6 Ga intersects the single highly unradiogenic $\varepsilon_{Hf(\sim 700\ Ma)}$ value observed in the Manhattan Schist sample from the Laurentian Margin (Fig. 6).

While it is geodynamically implausible that detridus geospatially related to the Kaapvaal-Zimbabwe cratonic suture zone was present within the sedimentary protolith of the Manhattan Schist, the observation described above illustrates the possibility that some of its sedimentary protolith zircons were derived from a re-worked terrane older than any of the crust exposed in the NJH. Archean rocks are located hundreds of km to the northwest of the study area (e.g. west of the Grenville front shown on Fig. 1), and Archean detridal zircons do appear in sedimentary basins northeast of the study area (e.g. the Newfoundland Appalachians; Cawood and Nemchin (2001)). However, the single highly unradiogenic zircon from the Manhattan Schist does not yield an Archean age. Instead, the fact that it is discordant, yielding a $^{206}Pb/^{238}U$ age of ~674 Ma and a $^{207}Pb/^{206}Pb$ age of ~1.9 Ga (data provided in electronic appendices 'A' and 'B') could mean that this zircon was derived from ancient crust (>1.9 Ga) that experienced re-working at ~700 Ma.

However, because there are no zircons with similar U–Pb age and Hf isotope systematics in either of the two tillite samples (PI-01 and LW-03), there does not appear to be a terrane with the requisite zircon U–Pb age and Hf isotope characteristics exposed along the portions of the Laurentian margin that were sampled by the advancing continental ice sheets during the Late Cenozoic. Therefore, future efforts to understand the tectonic relationship of the rocks in the Manhattan Prong to those of the Mesoproterozoic basement exposed to the west of the Ramapo Fault (Fig. 1) should first focus on thoroughly characterizing the U–Pb age and Hf isotope systematics of detridal zircons in the Manhattan Prong's metasedimentary units.

7. Conclusions

The new zircon U–Pb and Hf isotope data in this study support the following conclusions:

1) The Mesoproterozoic arc crust examined in this study originated as magmas with depleted mantle-like Hf isotope signatures beginning at ~1.4 Ga. This juvenile arc crust then evolved along an array with $^{176}Lu/^{177}Hf$ ranging from 0.022 to 0.005, as evidenced by the unradiogenic Hf isotope compositions observed in the re-worked products of the juvenile arc crust.
2) The nearly chondritic Hf isotope compositions of Late Ordovician aged magmas produced by partial melting of the lithospheric mantle can be explained by subduction-related contamination of the mantle wedge during the Mesoproterozoic. Calculations demonstrate that this lithospheric mantle source had a $^{176}Lu/^{177}Hf$ of ~0.022, which is similar to other mafic crustal reservoirs proposed in the literature.
3) A preliminary dataset from the Manhattan Schist suggests that while most of its zircons were derived from nearby crust, zircons derived from much more ancient crust may also be present. This highlights the need for a more extensive study of Manhattan Prong within an initial focus on the provenance of zircons in the metasedimentary units.

Supplementary data to this article can be found online at http://dx.doi.org/10.1016/j.lithos.2016.11.023.

Acknowledgements

This work was funded through institutional funds from the American Museum of Natural History to N. Alex Zirakparvar.

References

Alavi, M., 1975. Geology of the Bedford Complex and Surrounding Rocks, Southeastern New York. Contribution 24. Geology Department, University of Massachusetts, Amherst.
Amelin, Y., Lee, D.-C., Halliday, A.N., Pidgeon, R.T., 1999. Nature of the Earth's earliest crust from hafnium isotopes in single detrital zircons. Nature 399, 252–255.
Asmerom, Y., Patchett, J., Damon, P.E., 1991. Crust–mantle interaction in continental arcs: inferences from the Mesozoic arc in the southwestern United States. Contributions to Mineralogy and Petrology 107, 124–134.
Bartholomew, M.J., VanArsdale, R.B., 2013. Structural controls on intraplate earthquakes in the eastern United States. Geological Society of America Special Papers 493, 165–189.
Baum, E.M., Knox, H.D., Miller, T.R. (Eds.), 2002. Nuclides and Isotopes, 16th ed. Knolls Atomic Power Laboratory, Lockheed Martin (88 pp.).
Blackburn, T.J., Olsen, P.E., Bowring, S.A., McLean, N.M., Kent, D.V., Puffer, J., McHone, G., Rasbury, E.T., El-Touhami, M., 2013. Zircon U–Pb geochronology links the end-Triassic extinction with the central Atlantic magmatic province. Science 340, 941–945.
Blichert-Toft, J., Albarède, F., 2008. Hafnium isotopes in Jack Hills zircons and the formation of the Hadean crust. Earth and Planetary Science Letters 265, 686–702.
Bouman, C., Deerberg, M., Schwieters, J.B., 2009. Neptune and Neptune Plus: breakthrough in sensitivity using a large interface pump and new sample cone. ThermoFisher Scientific, application note: 30187. Accessed online at: http://www.cetac.com/pdfs/AN30187.pdf.
Bouvier, A., Vervoort, J.D., Patchett, P.J., 2008. The Lu-Hf and Sm-Nd isotopic composition of CHUR: constraints from unequilibrated chondrites and implications for the bulk composition of terrestrial planets. Earth and Planetary Science Letters 273, 48–57.
Cawood, P.A., Nemchin, A.A., 2001. Paleogeographic development of the east Laurentian margin: constraints from U–Pb dating of detridal zircons in the Newfoundland Appalachians. Geological Society of America Bulletin 113, 1234–1246.
Cecil, M.R., Gehrels, G., Ducea, M.N., Patchett, P.J., 2011. U--Pb-Hf characterization of the central Coast Mountains batholith: implications for petrogenesis and crustal architecture. Lithosphere 3, 247–260.
Chu, N.C., Taylor, R., Chavagnac, V., Nesbitt, R., Boella, R., Milton, J., German, C., Bayon, G., Burton, K., 2002. Hf isotope ratio analysis using multi-collector inductively coupled plasma mass spectrometry: an evaluation of isobaric interference corrections. Journal of Analytical Atomic Spectrometry 17, 1567–1574.
Condie, K.C., Belousova, E., Griffin, W.L., Sircombe, K.N., 2009. Granitoid events in space and time: constraints from igneous and detrital zircon age spectra. Gondwana Research 15, 228–242.
Corfu, F., Hanchar, J.M., Hoskin, P.W.O., Kinny, P., 2003. Atlas of zircon textures. Reviews in Mineralogy and Geochemistry. http://dx.doi.org/10.2113/0530469.
Drake, A.A., Volkert, R.A., Monteverde, D.H., Herman, G.C., Houghton, H.F., Parker, R.A., Dalton, R.F., 1996. Bedrock Geologic Map of Northern New Jersey. U.S. Geological Survey Miscellaneous Geologic Investigations Map I-2540-A.
Dunning, G.R., Hodych, J.P., 1990. U/Pb zircon and baddeleyite ages for the Palisades and Gettysburg sills of the northeastern United States: implications for the age of the Triassic/Jurassic boundary. Geology 18, 795–798.
Eby, G.N., 2004. Petrology, geochronology, mineralogy, and geochemistry of the Beemerville alkaline complex, northern New Jersey. In: Puffer, J.H., Volkert, R.A. (Eds.), Neoproterozoic, Paleozoic, and Mesozoic Intrusive Rocks of Northern New Jersey and Southeastern New York. Twenty-First Annual Meeting Geological Association of New Jersey, Mahwah, NJ, pp. 52–68.
Fisher, C.M., Vervoort, J.D., DuFrane, S.A., 2014b. Accurate Hf isotope determinations of complex zircons using the 'laser ablation split stream' method. Geochemistry, Geophysics, Geosystems 15, 121–139.
Fisher, C.M., Vervoort, J.D., Hanchar, J.M., 2014a. Guidelines for reporting zircon Hf isotopic data by LA-MC-ICPMS and potential pitfalls in the interpretation of these data. Chemical Geology 363, 125–133.
Fisher, C.M., Hanchar, J.M., Samson, S.D., Dhuime, B., Blichert-Toft, J., Vervoort, J.D., Lam, R., 2011. Synthetic zircons doped with hafnium and rare earth elements: a reference material for in situ hafnium micro analysis. Chemical Geology 286, 32–47.

Gehrels, G.E., Valenica, V.A., Ruiz, J., 2008. Enhanced precision, accuracy, efficiency, and spatial resolution of U–Pb ages by laser ablation-multicollector-inductively coupled plasma-mass spectrometry. Geochemistry, Geophysics, Geosystems 9:Q03017. http://dx.doi.org/10.1029/2007GC001805.
Goodge, J.W., Vervoort, J.D., 2006. Origin of Mesoproterozoic A-type granites in Laurentia: Hf isotope evidence. Earth and Planetary Science Letters 243, 711–731.
Guitreau, M., Blichert-Toft, J., 2014. Implications of discordant U–Pb ages on Hf isotope studies of detridal zircons. Chemical Geology 385, 17–25.
Guitreau, M., Blichert-Toft, J., Martin, H., Mojzsis, S.J., Albarede, F., 2012. Hf isotope evidence from Archean granitic rocks for a deep-mantle origin of continental crust. Earth and Planetary Science Letters 211–223.
Hall, L.M., 1975. Preliminary correlation of rocks in Southwestern Connecticut. Geological Society of America Memoirs 148, 337–350.
Hawkesworth, C.J., Dhuime, B., Pietranik, A.B., Cawood, P.A., Kemp, A.I.S., Storey, C.D., 2010. The generation and evolution of the continental crust. Journal of the Geological Society 167, 229–248.
Henry, A., 1997. Petrologic and Fluid Inclusion Constraints on the Tectonic Evolution of the Manhattan Prong, Southeastern New York. Virginia Polytechnic Institute and State University, Department of Geological Sciences (MS Thesis).
Hu, Z., Liu, Y., Gao, S., Liu, W., Zhang, W., Tong, X., Lin, L., Zong, K., Li, M., Chen, H., Zhou, L., Yang, L., 2012. Improved in situ Hf isotope ratio analysis of zircon using newly designed X skimmer cone and jet sample cone in combination with the addition of nitrogen by laser ablation multiple collector ICP-MS. J Analytical Atomic Spectrometry 27, 1391–1399.
Kemp, A.I.S., Foster, G.L., Schersten, A., 2009. Concurrent Pb–Hf isotope analysis of zircon by laser ablation multi-collector ICP-MS, with implications for the crustal evolution of Greenland and the Himalayas. Chemical Geology 261, 244–260.
Kemp, A.I.S., Wilde, S.A., Hawkesworth, C.J., Coath, C.D., Nemchin, A., Pidgeon, R.T., Vervoort, J.D., DuFrane, S.A., 2010. Hadean crustal evolution revisited: new constraints from Pb-Hf isotope systematics of the Jack Hills zircons. Earth and Planetary Science Letters 296, 45–56.
Laurent, O., Zeh, A., 2015. A linear Hf isotope-age array despite different granitoid sources and complex Archean geodynamics: example from the Pietersburg block (South Africa). Earth and Planetary Science Letters 430, 326–338.
Li, X.H., Faure, M., Lin, W., 2014. From crustal anatexis to mantle melting in the Variscan orogen of Corsica (France): SIMS U–Pb zircon age constraints. Tectonophysics 634, 19–30.
Li, X.H., Li, Z.X., He, B., Wang, X.C., 2012. The early Permian active continental margin and crustal growth of the Cathaysia Block: in situ U-Pb, Lu-Hf and O isotope analyses of detridal zircons. Chemical Geology 328, 195–207.
Li, H., Long, W.G., Li, Q.L., Liu, Y., Zheng, Y.F., Yang, Y.H., Chamberlain, K.R., Wan, D.F., Guo, C.H., Wang, X.C., Tao, H., 2010. Penglai zircon megacrysts: a potential new reference material for microbeam determination of Hf-O isotopes and U–Pb age. Geostandards and Geoanalytical Research 34, 117–134.
Long, L.E., Kulp, J.L., 1958. Age of the metamorphic of the rocks of the Manhattan Prong. Geological Society of America Bulletin 69, 603–605.
Long, L.E., Kulp, J.L., 1962. Isotopic age study of the metamorphic history of the Manhattan and Reading Prongs. Geological Society of America Bulletin 73, 969–996.
Ludwig, K.R., 2012. IsoPlot 3.75: A Geochronological Toolkit for Microsoft Excel. Berkeley Geochronology Center Special Publication No. 5, Berkeley, CA.
McLelland, J.M., Selleck, B.W., Bickford, M.E., 2010. Review of the Proterozoic evolution of the Grenville Province, its Adirondack outlier, and the Mesoproterozoic inliers of the Appalachians. Geological Society of America Memoirs 206, 1–29.
Merguerian, C., 1983. Tectonic significance of Cameron's line in the vicinity of the Hodges Complex; an imbricate thrust model for western Connecticut. American Journal of Science 283, 341–368.
Mose, D.G., Hayes, J., 1975. Avalonian igneous activity in the Manhattan Prong, southeastern New York. GSA Bulletin 86, 929–932.
Mose, D.G., Ratcliffe, N.M., Odom, A.L., Hayes, J., 1975. Rb-Sr geochronology and tectonic setting of the Peekskill pluton, southeastern New York. Geological Society of America Bulletin 87, 361–365.
Naeraa, T., Schersten, A., Rosing, M.T., Kemp, A.I.S., Hoffman, J.E., Kokfelt, T.F., Whitehouse, M.J., 2012. Hafnium isotope evidence for a transition in the dynamics of continental growth 3.2 Gyr ago. Nature 485, 627–630.
Nemchin, A.A., Pidgeon, R.T., Whitehouse, M.J., 2006. Re-evaluation of the origin and evolution of N4.2 Ga zircons from the Jack Hills metasedimentary rocks. Earth and Planetary Science Letters 244, 218–233.
Paige, S., 1955. Cambro-Ordovician age of the 'Inwood' limestone and 'Manhattan' schist near Peeksill, New York. Geological Society of America Bulletin 67, 391–394.
Patchett, P.J., Tatsumoto, M., 1980. A routine high-precision method for Lu-Hf isotope geochemistry and chronology. Contributions to Mineralogy and Petrology 75, 263–267.
Patchett, P.J., Kuovo, O., Hedge, C.E., Tatsumoto, M., 1981. Evolution of the continental crust and mantle heterogeneity: evidence from hafnium isotopes. Contributions to Mineralogy and Petrology 78, 279–297.
Prucha, J.J., 1956. Stratigraphic relationships of the metamorphic rocks in southeastern New York. American Journal of Science 254, 672–684.
Ratcliffe, N.M., 1981. Cortlandt-Beemerville magmatic belt: a probably late Taconian alkalic cross trend in the central Appalachians. Geology 9, 329–335.
Ratcliffe, N.M., Tucker, R.D., Aleinikoff, J.N., Amelin, Y., Merguerian, C., Panish, P.T., 2012. U–Pb zircon and titanite ages of late- to Post-tectonic intrusions of the Cortlandt-Beemerville Magmatic Belt, CN, NY, and NJ: relation to Iapetan closure in the Taconian orogeny. Geological Society of America Abstracts with Programs 44, 73
Roberts, N.M.W., Spencer, C.J., 2015. The zircon archive of continent formation through time. The Geological Society, London, Special Publications 389, 197–225.
Rudnick, R.L., Gao, S., 2003. Composition of the continental crust. In: Rudnick, R.L. (Ed.), The CrustTreatise on Geochemistry vol. 3. Elsevier, Amsterdam, pp. 1–64.
Slama, J., Kosler, J., Condon, D.J., Crowley, J.L., Gerdes, A., Hanchar, J.M., Hortwood, M.S.A., Morris, G.A., Nasdala, L., Norberg, N., Schaltegger, U., Schoene, B., Tubrett, M.N., Whitehouse, M.J., 2008. Plesovice zircon-a new natural reference material for U–Pb and Hf isotopic microanalysis. Chemical Geology 249, 1–35.
Solgadi, F., Moyen, J.F., Vanderhaeghe, O., Sawyer, E.W., Reisber, L., 2007. The role of crustal anatexis and mantle-derived magmas in the genesis of synorogenic Hercynian granites of the Livradrois area, French Massif Central. The Canadian Mineralogist 45, 581–606.
Spencer, C.J., Kirkland, C.L., Taylor, R.M., 2016. Strategies towards statistically robust interpretations of in situ U–Pb zircon geochronology. Geoscience Frontiers. http://dx.doi.org/10.1016/j.gsf.2015.11.006.
Stanford, S.D., 2005. Surficial Geology of the Caldwell Quadrangle, Essex and Morris Counties, New Jersey. Open File Map No. 66.
Stone, B.D., Stanford, S.D., Witte, R., 2002. Surficial geologic map of northern New Jersey. US Geological Survey Miscellaneous Investigation Map I-2540-L, scale 1:100,000.
Vervoort, J.D., Blichert-Toft, J., 1999. Evolution of the depleted mantle: Hf isotope evidence from juvenile rocks through time. Geochimica et Cosmochimica Acta 63, 533–556.
Vervoort, J.D., Patchett, P.J., Söderlund, U., Baker, M., 2004. Isotopic composition of Yb and the determination of Lu concentrations and Lu/Hf ratios by isotope dilution using MC-ICPMS. Geochemistry, Geophysics, Geosystems 5. http://dx.doi.org/10.1029/2004GC000721.
Volkert, R.A., 2012. Bedrock Geologic Map of the Booton Quadrangle, Morris County, New Jersey. NJ Geological Survey Open File Map Series OFM 95.
Volkert, R.A., Drake, A.A., 1999. Geochemistry and stratigraphic relations of Middle Proterozoic rocks of the New Jersey highlands. In: Drake Jr., A.A. (Ed.), Geologic Studies in New Jersey and Eastern Pennsylvania: US Geological Survey Professional Paper 1565C (77 pp.).
Volkert, R.A., Aleinikoff, J.N., Fanning, C.M., 2010. Tectonic, magmatic, and metamorphic history of the New Jersey highlands: new insights from SHRIMP U–Pb geochronology. Geological Society of America Memoirs 206, 307–346.
Wiedenbeck, M., Alle, P., Corfu, F., Griffin, W.L., Meier, M., Oberli, F., VonQuadt, A., Roddick, J.C., Spiegel, W., 1995. Three natural zircon standards for U-Th-Pb-, Lu-Hf, trace element, and REE analyses. Geostandards Newsletter 19, 1–23.
Withjack, M.O., Schilsche, R.W., Malinconico, M.L., Olsen, P.E., 2013. Rift-basin development: lessons from the Triassic-Jurassic Newark Basin of eastern North America. Geological Society of London, Special Publication 369, 301–321.
Zeh, A., Gerdes, A., Barton, J.M.J., 2009. Archaean accretion and crustal evolution of the Kalahari craton-the zircon age and Hf isotope record of granitic rocks from Barberton/Swaziland to the Francistown arc. Journal of Petrology 50, 933–966.
Zeh, A., Gerdes, A., Barton, J.M.J., Klemd, R., 2010. U-Th-Pb and Lu-Hf systematics of zircon from TTG's, leucosomes, meta-anorthosites and quartzite's of the Limpopo Belt (South Africa): constraints for the formation, recycling and metamorphism of Palaeorchaean crust. Precambrian Research 179, 50–68.
Zeh, A., Gerdes, A., Klemd, R., Barton, J.M.J., 2007. Archeaen to Proterozoic crustal evolution in the central zone of the Limpopo Belt (South Africa-Botswana): constraints from combined U–Pb and Lu-Hf isotope analyses of zircon. Journal of Petrology 48, 1605–1639.
Zeh, A., Gerdes, A., Klemd, R., Barton, J.M.J., 2008. U–Pb and Lu-Hf isotope record of detridal zircon grains from the Limpopo Belt-evidence for crustal recycling at the Hadean to early Archaean transition. Geochimica et Cosmochimica Acta 72, 5304–5329.
Zirakparvar, N.A., 2015. Cathodoluminescence guided zircon Hf isotope depth profiling: mobilization of the Lu-Hf isotope system during (U)HP rock exhumation in the Woodlark Rift, Papua New Guinea. Lithos 220-223, 81–96.
Zirakparvar, N.A., Mathez, E.A., Scoates, J.A., Wall, C.J., 2014. Zircon Hf isotope evidence for an enriched mantle source for the Bushveld Igneous Complex. Contributions to Mineralogy and Petrology 168. http://dx.doi.org/10.1007/s00410-014-1050-2.